MiKlip II – report about the use of the computing resources 2017

Project for report: **Project 807 – MiKlip II all modules**

Project lead: **Jochem Marotzke**

Project manager: **Sebastian Hettrich**

Report period: **01.01.2017 – 31.10.2017**

I. MiKlip Overview and allocated computing resources for 2017

The German Federal Ministry for Education and Research has since 2011 funded a comprehensive national program on decadal climate prediction, MiKlip (Marotzke et al. 2016). A second phase, MiKlip II, has been approved until 2019 and started on 1 October 2015, building upon MiKlip to further improve the central decadal climate prediction system and by the end of the project to transfer the system for operational use to the German meteorological service DWD. The successful improvement and thus application of the prediction system depends on ongoing research of new initialisation, ensemble perturbations, and bias correction strategies that must be tested and, if applicable, incorporated into the prediction system. Furthermore, model resolution must be increased, which has been shown to improve the representation particularly of atmospheric processes, the limited representation of which currently reduces the forecast skill over continental areas.

The aim of MiKlip II is thus to further improve the decadal prediction system that was established during the first project phase, with the ultimate aim to provide a system that can be used operationally by the DWD. All five MiKlip modules (respectively represented in the projects below) work towards this aim with different research focusses, thereby making strong use of resources provided by the DKRZ, both through computing time allocated on shared resources and through the MiKlip Server.

Before 2017, the partners of the second phase of MiKlip (MiKlip II) have applied for computing time via the following five projects:

- project bu0801: MiKlip II Module A – Determination of initial conditions and initialisation,
- project bm0764: MiKlip II Module B – Processes and Modelling
- project bb0849: MiKlip II Module C – Regionalisation of Decadal Predictions
- project bm0807: MiKlip II Module D – Synthesis, and
- project bb0763: MiKlip II Module E – Evaluation of the MiKlip Decadal Prediction System.

The allocated times for 2017 including the additional allocations for quartal 3 and 4 are shown in table I. As of now (17th October), on average 80% of the allocated node hours for 2017 have been used for all the 5 different MiKlip modules.

Table I; Allocations for 2017

Project Number	Project Name	Mistral compute time [Node hours]	Lustre work [GiB]	HPSS arch [GB]	HPSS doku [GB]
bu0801	Module A	220527	296901	320884	0
bm0764	Module B	261179	222956	469639	38748
bb0849	Module C	1094274	197791	2347736	5627
bm0807	Module D	1203827	479297	781894	0
bb0763	Module E	34940	45511	457079	11254
bm0769	ALARM*	0	15.000	5.000	5.000
Sum ALL MiKlip		**2814747**	**1257456**	**4382232**	**60629**

* This project was not part of the 2017 application, but still was bundled under “all MiKlip”, thus it is included here for completeness in this table.

II. Table of content

1. Module A – Initialisation

Project **bu0801**

Project title: **MiKlip II Module A: Determination of initial conditions and initialisation**

Project leader: **Johanna Baehr** (CEN, UHH), **Andreas Hense** (Meteorologisches Institut University Bonn), **Stefan Hagemann** (MPI-M), **Detlef Stammer** (CEN, UHH)

Reporting period: **01.01.2017 – 31.10.2017**

1.1 Module A – Coordination2

Table 1.1: Computational resources used during the report time

Planned	Granted	Used by mid-September 2017	Comments
SUM of Node-h: 23000	13800 (60%)	5282	Other computing resources were used for planned hindcasts so that AODA-PENG-Bonn can run their experiments
SUM of disk space on work: 12000 GiB on	6000 (50%)	8530	

Scientific activities conducted during the report time 2017

To deal with model biases and initialisation shocks in the MiKlip prediction system (based on the MPI-ESM in LR configuration) for decadal climate predictions, we have been testing a new initialisation method, which aims to reduce model initialisation shock by filtering out the modes from initial conditions which cannot be represented by the climate model.

To produce initial conditions for decadal predictions, a nudging run over 1960-2015 was performed, where temperature and salinity fields were nudged toward filtered ORAS4 anomalies added to MPI-ESM climatology (derived from the historical simulation). The nudging routine uses a relaxation time-scale of 11 days. To be consistent with the previous development stage of the MiKlip Project, the initialised hindcasts are started from the end of October. Also the modes of variability from the prediction system are derived for Octobers and consequently assimilated into MPI-ESM only during October (MODES-ASSIM). To analyse how this approach differs from the traditional one (nudging during every month), we carried out an assimilation run with nudging non-filtered state in Octobers only (ANON-1m-ASSIM) and compared it to the pre-operational assimilation run (here called as ANON-12m-ASSIM). To test the performance of the new climate-modes initialisation scheme as compared to anomaly initialisation method, we performed 2 sets of initialised hindcasts (10-years long) with 10 ensemble members initialised over the period 1960 to 2015 (+tests ~200000 Node-h).

For AMOC skill, the role of initialisation is essential. ANOM-1m-INIT (see Figure) and ANOM-12m-INIT (not shown) demonstrate basin-wide skill with the lesser RMS errors up to lead years 5-6. While the skill from anomaly initialised hindcasts decreases gradually with time, MODES-INIT shows rather lead-time independent correlation skill, which is mostly limited to the high latitudes. Also RMS errors do not grow as much with lead years as in ANOM-1m-INIT or ANOM-12m-INIT (Figure 1.1). Overall, new initialisation method indicates more persistent skill in high latitudes, but loss of skill in the tropics. Underlying mechanisms are investigated.

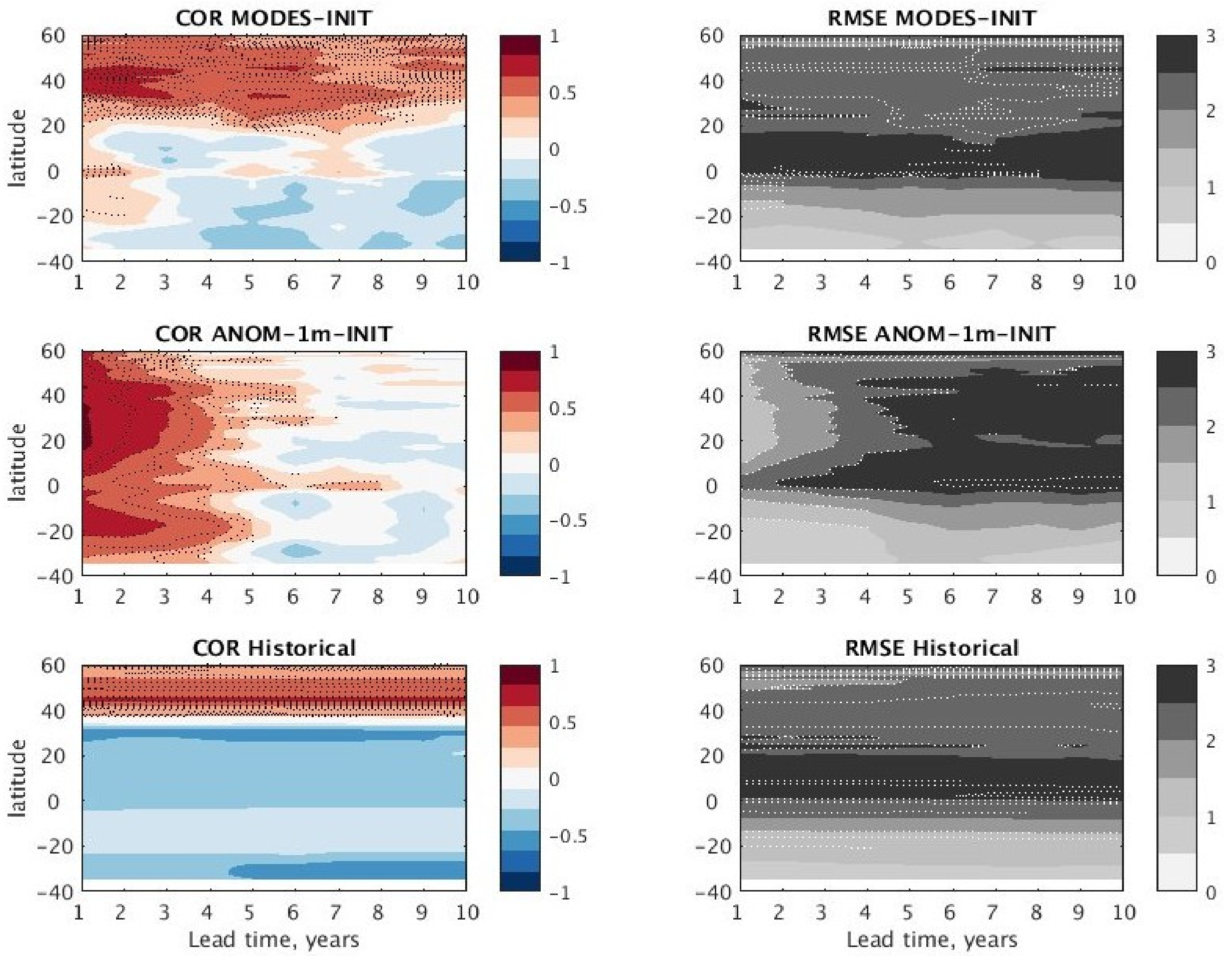

Figure 1.1: AMOC skill with respect to original ocean reanalysis in terms of correlation coefficients (left panels) and root-mean squared errors (right panels, in SV).

1.2 Module A – WP2 PastLand2

During the last year, PastLand2 investigated the sensitivity of the MPI-ESM 1.2.00 to soil moisture assimilation. Furthermore, we run a number of test cases and did revisions for the land surface assimilations scheme, which was developed and implemented into MPI-ESM during the first year of PastLand2.

By now, the assimilation scheme is thoroughly tested (using artificial soil moisture observations constructed from a reference simulation) and performs as expected. Figure 1.2.1 demonstrates how assimilated dry soil moisture perturbations travel through the soil column and accumulated in the deep layers, which agrees with the findings in an earlier initialisation study (Stacke & Hagemann, 2016).

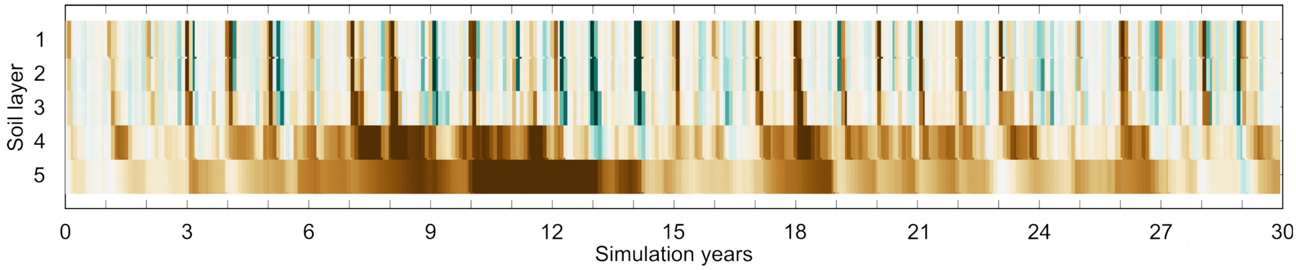

Figure 1.2.1: Migration of an assimilated top layer soil moisture anomaly through the soil column. For better comparability, the moisture variation in every soil layer is normalised by the range of its values, with brown and green colours to indicate dry and wet anomalies, respectively.

Our sensitivity studies revealed that assimilation in the fully coupled model set-up may result in severe issues, namely the violation of the water balance by artificially adding or subtracting water in a closed system. If extreme wet or dry soil moisture states are assimilated, the corresponding signal will end up in the ocean and may change the sea level by up to 1m during a 30 years long simulation. While the assimilation of observed anomalies are expected to be far less extreme, this finding already demonstrates the need to adapt the general assimilation set-up, e.g. by merging ocean and land states from different assimilation runs.

In order to analyse the model sensitivity to the assimilation of extreme soil moisture states without interference from sea level change, we developed a special test set-up. Here, we did not use global fields consisting of either wet or dry soil moisture states, but merged both to create a dataset with a wet tropical belt and dry extra-tropics and vice versa (see figure. 1.2.2). In this way, the sum of global soil moisture anomalies compared to the reference simulation equals zero and the effects on the sea level during the simulation time are strongly reduced.

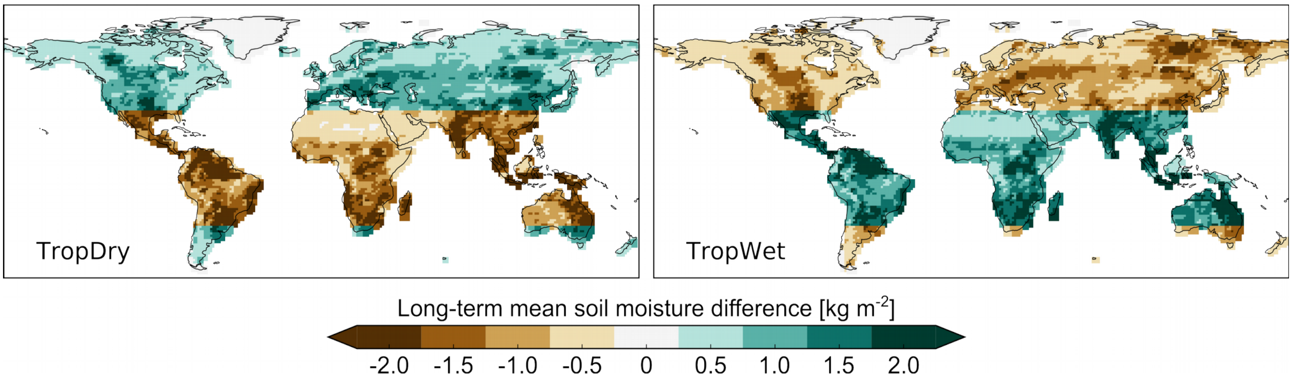

Figure 1.2.2: Mean long-term difference between the constructed soil moisture assimilation fields and the reference simulation.

Using an ensemble of 5 simulations per experiment for a 30 years period, we identified two main pathways in which the soil moisture perturbation affects the global model. The largest signal is transported through evapo-transpiration, which affects the global surface temperature and atmospheric moisture content, ultimately leading to alteration of precipitation. Secondly, soil moisture anomalies modify land surface run-off and therefore river discharge, resulting in changes in sea surface salinity (Fig. 1.2.3).

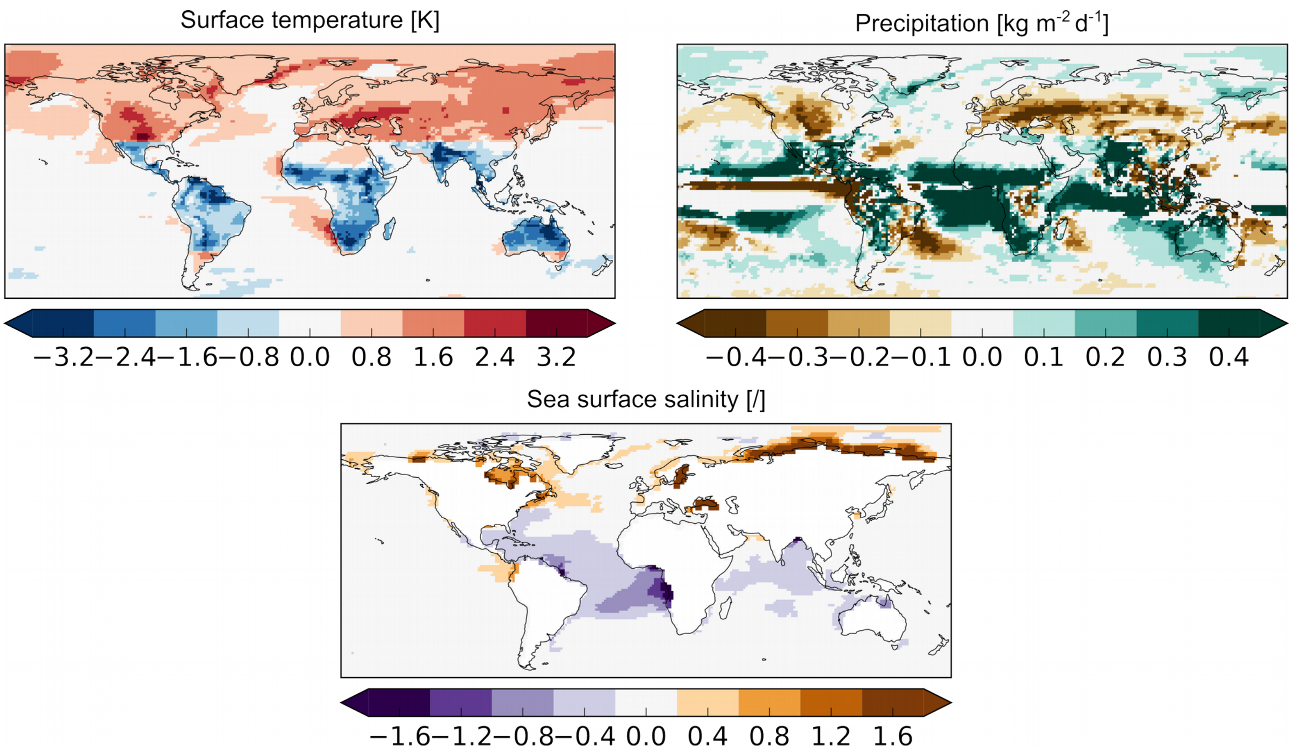

Figure 1.2.3: Difference between both assimilation experiments, showing the effect of assimilating wet anomalies into the tropical belt and dry anomalies in the extra-tropics.

This sensitivity study not only demonstrates the general functionality and physical validity of the assimilation scheme, but also highlights the sensitivity of climate to the region of wet and dry anomalies. While both assimilation datasets agree with the reference simulation in terms of mean global soil moisture content, figure 1.2.4 demonstrates the changes in the hydrological cycle dependent on the latitude of the anomalies. While the wet anomalies in the tropics strongly increase evapo-transpiration and effectively transport the additional water into the ocean, wet anomalies in the extra-tropics are of little effect as the soil is wet anyway and evapo-transpiration is rather limited by available energy. Here, the dry anomalies in the tropics dominate evapo-transpiration change, resulting in decreased ET over the land surface and reduced water transport into the ocean. Note, that in both cases the sum of surface run-off change is negative, as its increase in regions with wet anomalies is usually smaller than its respective decrease in regions with dry anomalies. This results from the non-linear relation between root zone soil moisture and surface run-off in the MPI-ESM.

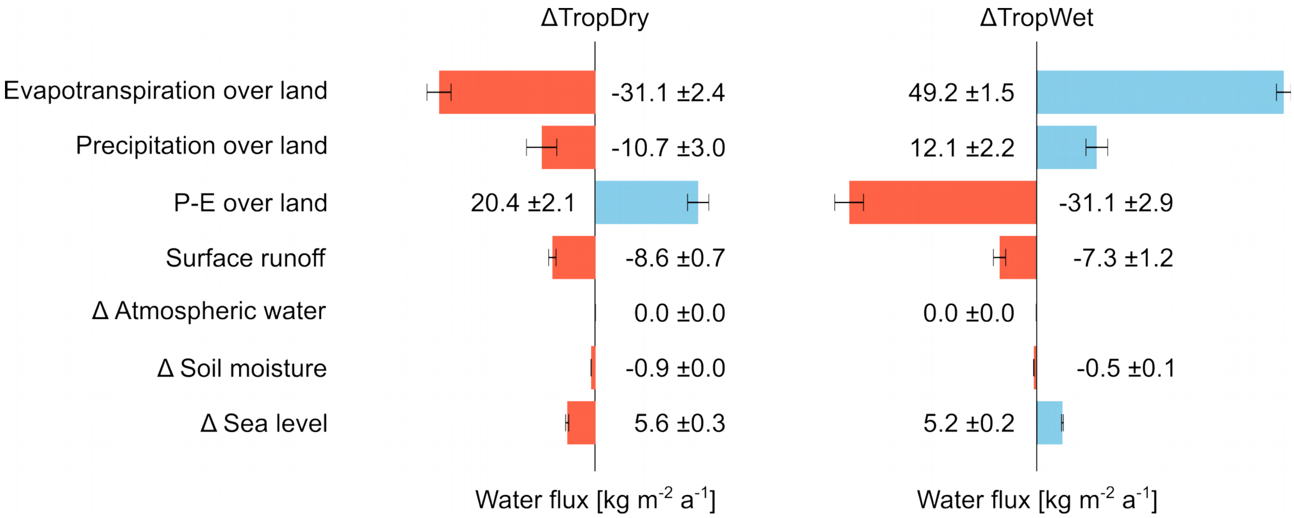

Figure 1.2.4: Changes in water fluxes and states between the assimilation experiments and the reference simulation.

Differences to last year's proposal

Last years proposal asked for computing time for test simulations with high temporal resolution in an AMIP set-up as well as a set of hind-cast simulations with the fully coupled MPI-ESM. As the AMIP simulations revealed the need to investigate the model sensitivity towards soil moisture assimilation also in the fully coupled system (due to sea level changes), we postponed the hind-cast simulations and conducted several ensemble simulations to evaluate the general validity of our assimilation approach. These ensembles used artificially constructed assimilation based on a reference ensemble.

The computing time required for the revision of the assimilation scheme as well as for the ensembles simulations conducted for several different sensitivity experiments accumulates to about 37000 Node h. From this amount only 5500 Node h were charged on the MiKlip2-Module A account to spare enough resources for other tasks within Module A in spite of the resource cuts compared to the original application.

In conclusion, our experiments consumed about 1.5 times as much computing time as requested in our original computing time application (25020 node h).

1.3 Module A – WP3 AODA-PENG2

WP3: Atmospheric and Oceanic Data Assimilation & Ensembles Generation (AODA-PENG2)
Scientific activities conducted during the report time

WP3.1 (University Bonn): Breeding techniques

The breeding technique for ensemble generation was tested on the MPIESM LR (T63L47/GR15L40) version of the model. We implemented a modified version of the classical bred vector method by Kalnay and Toth (1993). It is based (1) on velocity, temperature and salinity variables with the growth rate measured by a weighted total energy norm and (2) by iterating on a seasonal evolving but otherwise fixed ocean state. The breeding routines are externally designed and are able to be implemented in different coupled climate models through shell scripts. The routines do not depend on the model resolution and the time period of the iterative looping is defined by the user. Up to date the code is coupled to the LR (T63L47/GR15) model version. For 9 starting years, eight bred vectors were calculated on 12 months looping period over 5 iteration steps. The rescaling coefficients of the growing anomalies derived from the total energy norm and the change of global mean ocean temperature in the top layers between the iteration steps is investigated.

The total energy norm of the growing modes alone could not produce perturbation amplitudes comparable to the corresponding ones of the starting reanalysis. Therefore, the Bred Vectors were additionally constrained by applying a regression technique with the observations. This results in a coefficient which is based on the ratio between the covariance of the bred vectors with anomalies derived from observations and the energy norm of the Bred Vectors themselves. In this way realistic perturbation amplitudes scaled with observations were obtained. The resulting anomaly patterns are added to the initial fields and the unrealistic drift in the ensemble runs was avoided which occurred when using the pure, unscaled bred vectors.

Due to the requirements for the MiKlip Module A project recommendation statement at the end of 2017, it was necessary to perform a 56 years long hindcast experiment starting from the pre-operational reanalysis produced at DWD. A new adjustment of the model set-up was implemented, such that the perturbations were applied at 31st of October, instead of 31st of December. The 9 member hindcast was performed (figure 1.3.1) using 5 iterative steps to calculate the Bred Vectors with the observational scaling applied after these iterations. For this purpose, and together with the preliminary tests, around 100000 node hours and 51 TB on Mistral were used.

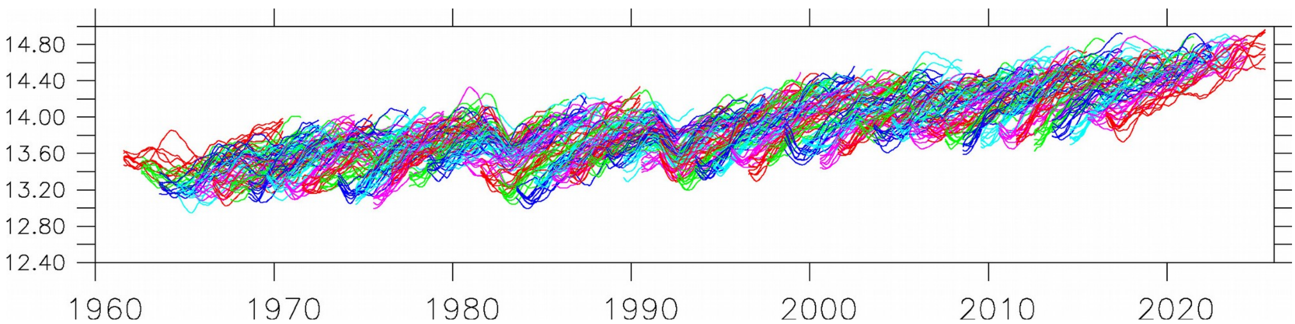

Figure 1.3.1: Hindcast produced with Bred Vectors, absolute values of ocean surface temperature for all ensemble members from 1961 until 2016

For the next year, we plan to perform the following:

a) Testing the amplitude of the ocean perturbations (sensitivity study):
   - investigating the amplitude and structure sensitivity of the bred vectors with respect to the number of iterations;
   - constructing orthogonal BV with positive and negative amplitudes such that the mean perturbation amplitude remain near the initial state;

b) BV routine development to include perturbation of the atmosphere, which are consistent with oceanic perturbations and test experiments of the atmospheric BV, and simultaneously perturbed atmosphere and ocean.

WP3.2 (University Hamburg): Oceanic EnKF assimilation

Within MiKlip2 Module A the work package 3.2 is concerned with the implementation of an EnKF scheme into the ocean component of the coupled Earth system model MPI-ESM to initialise decadal predictions. It is carried out at IfM Hamburg. We are using the "LR" setup of MPI-ESM, that is ECHAM6 T63L47 and MPIOM GR15 with 40 levels.

Summary of work carried out in 2017

The Ensemble Kalman Filter (EnKF) for MPIOM (MPI-ESM 1.0) has already been successfully implemented (Brune et al. 2015) in its global variant using the Parallel Data Assimilation Framework (PDAF, Nerger & Hiller 2013) in MiKlip phase I. In 2017 our work within MiKlip phase II aimed at a successful initialisation and simulation of hindcasts based on the improved weakly coupled assimilation system with PDAF/EnKF developed in 2016.

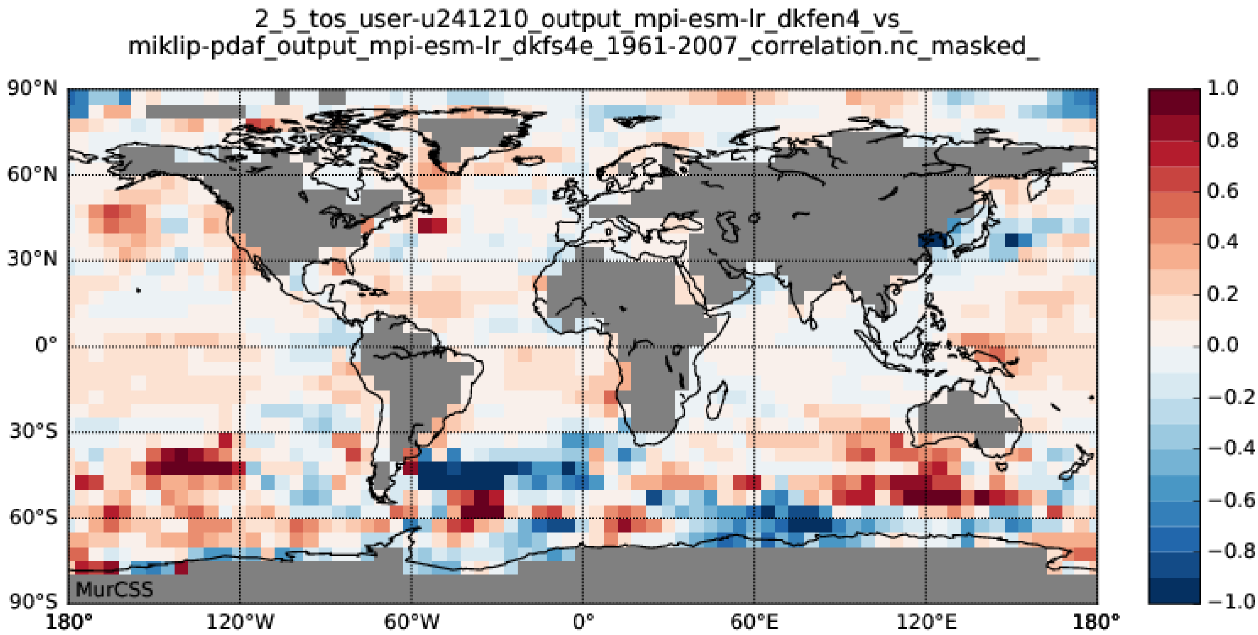

Figure 1.3.2: Difference in correlation skill of 1962-2012 mean lead year 2 to 5 sea surface temperature between hindcasts initialised by localised EnKF and global EnKF assimilation.

For the weakly coupled assimilation we designed and carried out a two step spin-up simulation: 300 years with one ensemble member and only atmospheric nudging and 50 years with 16 ensemble members with coupled assimilation of mean 1960s monthly climatology. This spin-up considerably reduces drifts in the deep ocean temperatures and the meridional overturning circulation. Based on the spin-up simulation we carried out a 16 member coupled assimilation for the time period 1958 to 2016: local EnKF assimilation with variable inflation of EN4 temperature and salinity profiles in the ocean and atmospheric full value nudging to ERA40/ERAInterim re-analysis. We initialised hindcasts from this assimilation starting at the 1st of November every year 1959 to 2016. Preliminary results show improved correlation skill for ocean sea surface temperature for these hindcasts when compared to hindcasts initialised by the simple EnKF assimilation used in MiKlip phase I, especially in the North Atlantic sub-polar gyre and the tropical Pacific (figure 1.3.2).

1.4 Comparison to 2017 requested

Allocated resources for 2017 have been used according to plan.

1.5 References

Brune, S., L. Nerger, J. Baehr, 2015: Assimilation of oceanic observations in a global coupled Earth system model with the SEIK filter, Ocean Modelling 96, Part 2, 254 – 264.

Nerger, L., Hiller, W., 2013. Software for ensemble-based data assimilation systems - Implementation strategies and scalability. Computers and Geosciences 55, 110 – 118

2. Module B – Processes and Modelling

Project: **bm0764**

Project Title: **MiKlip-II Module B: Processes and Modelling**

Module B coordinator: **Johann Jungclaus**

Sub-projects:

- **MOVIECLIP** (PIs: Johann Jungclaus, Jürgen Bader, Daniela Matei, Wolfgang Müller (MPI-M)),
- **ALARM-II** (Claudia Timmreck, Hauke Schmidt (MPI-M), Kirstin Krüger (Uni Oslo))
- **ATMOS-MODINI** (Richard Greatbatch (GEOMAR), Johann Jungclaus (MPI-M), Rüdiger Gerdes (AWI))
- **PROCUP** (Tatiana Ilyina, MPI-M)

Reporting period: **01.01.2018 – 31.10.2018**

2.1 ALARM-II

The central goal of the MiKlip ALARM project is to study the response of the climate system to volcanic aerosol perturbations and the effects of past historic volcanic eruptions. An assessment of the climate impact of large volcanic eruptions cannot be achieved without a deep understanding of post volcanic climate variability. This task can only be addressed in a multi-model framework as will be done in the CMIP6 Model Intercomparison Project on the climate response to Volcanic forcing (VolMIP). In VolMIP different time scales are considered: the seasonal-to-interannual atmospheric response to a 1991 Pinatubo-like volcanic eruption and the long-term (up to the decadal time scale) climate response to very strong volcanic eruptions, like the 1815 Tambora eruption.

For 2017, CMIP6 (Coupled Model Inter-comparison Project, Phase 6, Eyring et al., 2016) related work was anticipated but could not be carried out as the CMIP6 model set up was not finished. Instead we have concentrated on some preparatory work for VolMIP. We have tested the sensitivity of climate simulated by the MPI Earth system model to a range of volcanic forcings for the early 19th century constructed using estimated uncertainties in volcanic stratospheric injections and the volcanic forcing generator EVA (Toohey et al., 2016). Ensemble simulations have been performed (under project 764 and project 960) and compared to climate reconstructions.

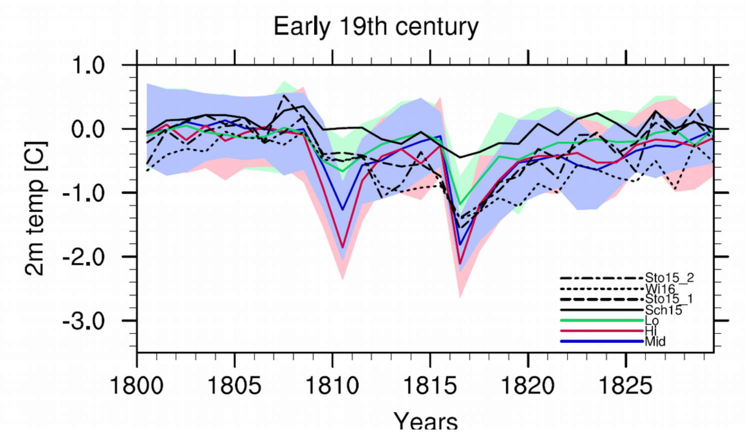

Figure 2.1: Northern Hemisphere summer land temperature anomalies simulated with the MPI-ESM using the three forcing reconstructions (Lo, Hi, Mid) based on the evolv2k reconstruction (Toohey and Sigl, 2017) compared to temperature reconstructions (Wi16: Wilson et al., 2016; Sch15: Schneider et al., 2015; Sto15_(1,2): Stoffel et al. (2015). The shaded regions indicate the envelope of the simulated anomalies.

Our results show that a combination of volcanic forcing and internal variability most likely led to the climate evolution of the early 19th century. The range of volcanic forcing uncertainties is similar to the range of internal variability. The reconstructed temperature anomalies lie in general, within the range of simulated temperature anomalies incorporating uncertainties in the volcanic forcing. However time between the two eruptions is colder and the signal of the 1809 eruption is weaker in the reconstruction.

2.2 ATMOS/MODINI

The MiKlip sub-project ATMOS-MODINI has two parts. ATMOS has the goal to alleviate the North Atlantic cold bias in the MPI-ESM with the view of testing the hindcast skill of the corrected model. In the MPI-ESM there is a large cold bias in North Atlantic sea surface (and subsurface down to 1000m) temperature, that we are attempting to correct using the flow field correction (FFC) method described in Drews et al. 2015. The FFC procedure consists of two main steps, (i) the interactive run, during which the correction is computed at each time step and (ii) the non-interactive run that uses a correction that has been diagnosed as a long-term monthly mean from the interactive run. In the reporting period, a number of sensitivity experiments have been conducted, including combinations of the FFC correction and surface freshwater correction during step (i) and experimentation with the region where the correction is applied in step (i) and (ii).

In the end, best results were obtained using a relatively small region during step (i), covering the Gulf Stream extension region and a larger region during step (ii), covering large parts of the North Atlantic. Freshwater flux correction in combination with the FFC method was found to have no significant influence and is not used in the following. The decrease in bias is shown in Figure 2.2.1, where the top panels show the typical cold bias (30-year mean) in the uncorrected model (CTL) referenced to the Levitus climatology and bottom panels show the same for the corrected model (FFN-ST5E). The cold bias is largely removed, also at depth (see right panels, showing the model level at 220 m depth), a small cold bias of about 1-2 K remaining at the surface.

Subsequently, both the uncorrected and the corrected runs were further integrated to obtain a long time series (700 and 1000 years, respectively) to analyse the decadal to multi-decadal variability of both model versions. In particular, we started analysing the Atlantic multi-decadal variability following the analyses of Drews and Greatbatch (2017), who find a much more realistic AMV in a corrected version of the Kiel Climate model than in the uncorrected version.

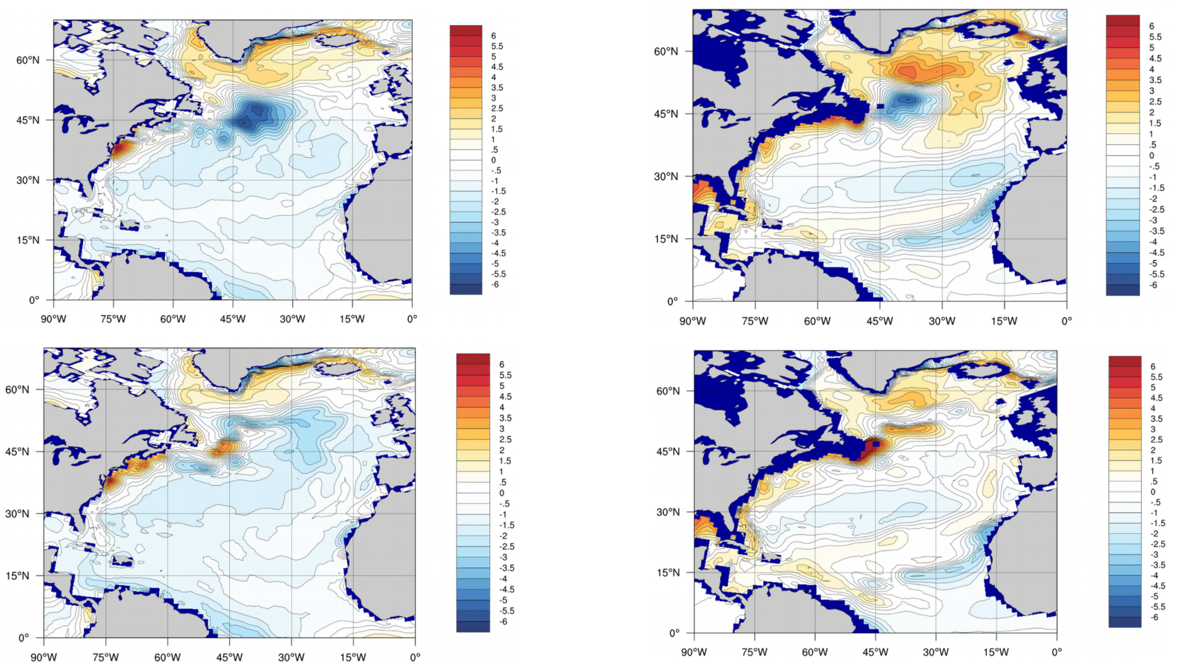

Figure 2.2.1: 30-year mean temperature bias from (top) a long PI-control (CTL) run and from (bottom) a corrected model version (see text for details). (left) showing the uppermost model level and (right) showing 220m depth. The contour interval is 0.5 K. Bias refers to the World Ocean Atlas (Levitus et al. 1998).

The MODINI part is to explore ways to improve the initialisation of the MiKlip system in the tropics. Thereby, MODINI uses reanalysis wind stress anomalies seen by the ocean model in the

coupled system to drive the initialisation run that is subsequently used for decadal hindcasts.
A suite of retrospective forecasts (hindcasts) has been completed, using an initialisation run driven by reanalysis wind stress anomalies added to the model climatological wind stress (MODINI), similar to Thoma et al. (2015). Here, the ERA-40 reanalysis has been used for the period 1958-1989 (ERA-Interim for 1990-2016). The hindcasts have been carried out as part of the joint effort within MiKlip II for the inter-comparison of initialisation methods.

In particular, three initialisation runs were integrated for the years 1958 – 2016. Subsequently, four hindcasts have been inialised (6-hourly lagged) from each initialisation run on November 1st of each year from 1959-2016, in total generating 12 ensemble members.
A preliminary result is shown in Figure 2.2.2, comparing the skill of MODINI with the MiKlip pre-operational (PreOp) system for 2-5 year lead-time in terms of the skill in hindcasting 2 m temperature verified against HadCRUT4 observations.
Surprisingly, MODINI skill is not distinguishable from that of the PreOp system in the tropical Pacific, where it is a priori thought to yield the largest improvements. Instead, at least for the period 1990 – 2011, MODINI has improved skill in the Atlantic and Indian Ocean sectors.

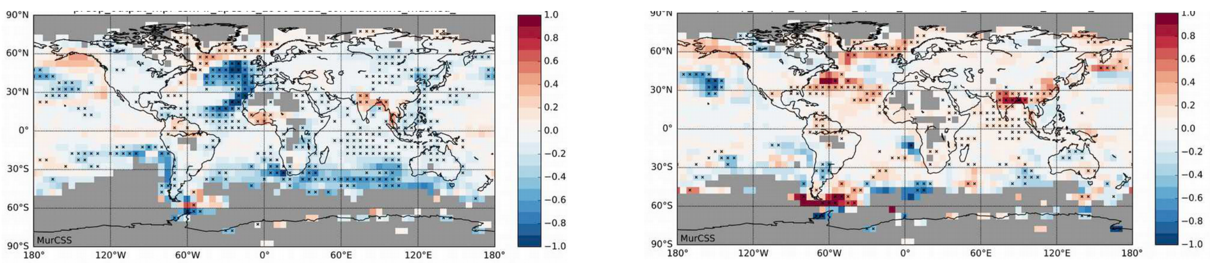

Figure 2.2.2: Difference between MODINI and PreOp hindcasts in ensemble mean correlation skill score of 2 m air temperature for the 2-5 year mean hindcasts evaluated against observations (HadCRUT4 ensemble mean). (left) for SY 1960 – 2011 and (right) for SY 1990-2011. Hatching marks significance based on Monte Carlo tests and grid points with insufficient observations are masked. Generated using the MurCSS plugin of the Central Evaluation System (CES, Kadow et al., 2015)

2.3 MOVIECLIP

MOVIECLIP aims at an assessment and improved representation of key oceanic and atmospheric processes in the MiKlip prediction system that are important for decadal predictability in the North Atlantic region and Europe. During the report period MOVIECLIP concentrated on continuing the analysis of the Atlantic Multi-decadal Variability (AMV) in the MPI Grand Ensemble that was started in 2016. The aim of this work is to get a better understanding of the mechanisms that control North Atlantic large-scale temperature variations on decadal time scales. Particularly we address the question, whether ocean dynamics is involved in controlling the AMV or whether the AMV is a mainly atmospherically driven mode. The MPI Grand Ensemble consists of a 2000-year pre-industrial control run, a 100-member ensemble of historical simulations covering the time period from 1850 to 2005 and a 68-member ensemble of 155 year long runs with an idealised forcing with an incremental $CO2$ increase by 1%/year.

We found strong statistical evidence that AMV has a regional component that is driven through ocean heat transport changes: The variability in the region east of Newfoundland substantially contributes to the AMV in observations, the pre-industrial control experiment and the historical ensemble (figure 2.3.1 (a)-(c)). In contrast, the AMV imprint on this region is much weaker in the ensemble with strong $CO2$ forcing (figure 2.3.1 (d)). Our analysis shows, that decadal ocean temperature variability in that region is mainly induced by ocean dynamics, and not by anomalous turbulent surface heat fluxes (dark blue lines in figure 2.3.2(a)). Temperature anomalies east of Newfoundland are preceded by anomalous Labrador Sea convection and, as a consequence, a southward propagating AMOC signal (figure 2.3.2(a)); therefore, the AMV might have a predictable component on these time-scales. Compared to the pre-industrial control experiment and the historical ensemble, the lag-correlations between Labrador Sea convection, AMOC and Northwest Atlantic temperature becomes weaker under strong $CO2$ forcing (figure 2.3.2(b)). Also, both, AMV and AMOC variability are strongly reduced in the ensemble with the forcing with an incremental $CO2$ increase by 1% per year. This might be partly explained by a reduced ability of the atmosphere to trigger convection variability in the Labrador Sea changes under strong $CO2$ forcing.

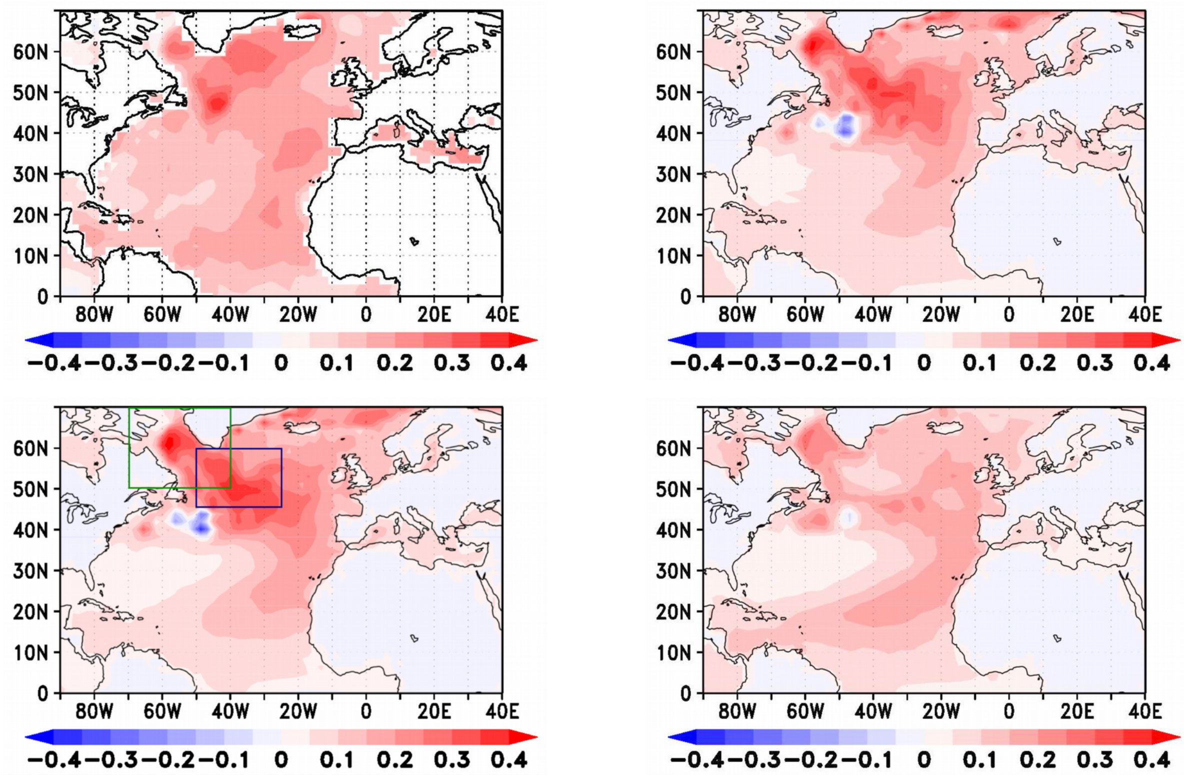

Figure 2.3.1: AMV pattern as regression of 10-year lowpass-filtered local SST on the AMV index, defined as the 10-year lowpass-filtered anomaly of the field mean SST averaged over the domain 85°W-20°E/0°-70°N (in K per standard deviation of the index) for (upper left) the HadISST, (upper right) the pre-industrial control simulation, (lower left) the historical ensemble and (lower right) the ensemble with an incremental CO2 increase by 1% /year.

The experiments we analysed were not performed within the bm0764 project, therefore we used less computing time than originally expected. However, for the large amount of data that go along with post-processing and analysing such a big ensemble, we benefited from the disc space that was granted to the project as well as from the opportunity to run a high number of post-processing tasks in parallel.

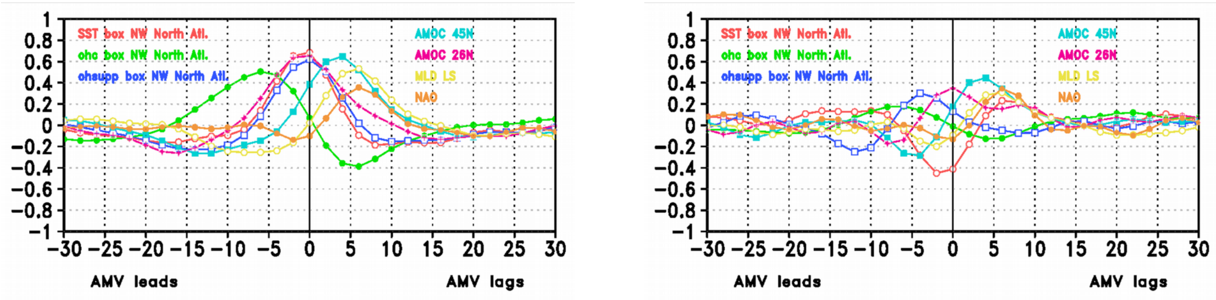

Figure 2.3.2: Lag cross-correlations between the AMV and different variables of North Atlantic climate variability for (left) the historical ensemble and (right) the ensemble with an incremental CO2 increase by 1%/year. The colours indicate the different indices, i.e. the local SST averaged for a box east of Newfoundland (red, 50°W-25°W/45°N-60°N, dark blue box in figure 2.3.1(c)), the vertically integrated ocean heat content (light green, averaged for the same box), the ocean heat supply as the vertically integrated ocean heat content change in the same box minus the turbulent heat flux integrated over the box's surface (dark blue), the AMOC at 45°N (cyan) and 26°N (magenta), the Labrador Sea mixed layer depth (averaged for a box 70°W-40°W/50°N-70°N, green box in figure 2.3.1(c)) and the NAO index as the leading principal component time series of North Atlantic (90°W-40°W/20°N-80°N) sea level pressure (orange). The horizontal axis indicates the lag in years, with the AMV leading (lagging) to the left (right). Before computing the correlations, a 10-year low-pass filter was applied to all indices.

Decadal climate prediction project component C (DCPP-C) experiments

In order to follow the DCPP-C protocol (Boer et al. 2016) two suggested methods for implementation of the SST for the pacemaker experiments the MPI-ESM-LR have been tested. For the first method the SST signal is restored directly to the model (nudging). For the second method the SST signal is imposed by altering surface fluxes. Outside of the restoring region, the model evolves freely, allowing a full climate system response. Previous publications have shown that SST restoring, especially in the Atlantic, may lead to undesirable effects on ocean currents and associated heat transport such as AMOC which may affect SSTs in other regions (including the South Atlantic) and which can obscure the results. Therefore a density correction was implemented into the model. However, with the method of altering surface fluxes the SST signal was not transferred back to the ocean component in a sufficient way and we have decided to use the relaxation method for the DCPP-C simulations. Due to a delay in the provision of the external CMIP6 forcing the climate model MPI-ESM-1.2-LR has become available only recently. Therefore we have started the DCPP-C simulations with a considerable delay. We expect that we will be able to finish 1/3 of the envisaged DCPP-C simulations in the remainder of 2017 and have to postpone 2/3 of the envisaged simulations to 2018.

2.4 PROCUP

The main goal of work package PROCUP is to improve the representation of the oceanic carbon cycle in the ocean biogeochemical component (HAMOCC) of MiKlip decadal prediction system and further assess the predictability of the oceanic carbon uptake. Our study can be summarised in the following 3 aspects regards to the model spin-up and the process understanding in variability and predictability of the oceanic carbon uptake.

I. Support Module D to reduce drift of oceanic carbon cycle due to data assimilation

In the current MiKlip assimilation system, we nudge the modelled ocean and atmosphere physical fields towards the reanalysis data. The ocean biogeochemical tracers show large drift as they adjust to the new ocean physical states, especially in the first 10-15 years of the assimilation run. We run several cycles of spin-up simulation with fixed atmospheric CO2 concentration for ocean biogeochemical component HAMOCC, to allow the model to slowly adjust to its new state. We have tried several ways to balance the strong up-welling of the nutrient and hence keep the ocean carbon uptake in a reasonable level. For the MiKlip pre-operational high-resolution model MPI-ESM-HR under CMIP6 forcing, we set up several parallelised simulations under different configuration (e.g., weathering rate, inventory adjustment, different length of cycle). In our final HAMOCC spin-up simulation, the MPI-ESM-HR is integrated in total for 46 years with nudging atmosphere and ocean physical fields, i.e., 2 cycles of 20-year simulations plus 6 years. In this spin-up simulation, the atm. CO2 concentration is fixed to the year 1958 level for HAMOCC. The silicate and dissolved inorganic carbon inventory are reduced globally according to the ratio of inventory between model and observations. The restart state of ocean biogeochemical fields from the spin-up run is provided to Module D as initial state of MPI-ESM-HR assimilation run. In the assimilation run, the evolution of all the ocean biogeochemical parameters is more stabilised; and the oceanic carbon uptake is in the right sign, i.e., the ocean is taking up carbon from the atmosphere.

II. Variability of the ocean carbon uptake

II.1 The prominent role of internal decadal variability in the current and near future oceanic CO2 uptake (GRL, under revision)

Observations (Fay and McKinley, 2013; Landschützer et al., 2015; Schuster and Watson, 2007) have revealed pronounced decadal variations occurring along with decreasing ocean carbon uptake for the period from 1992-2001. Understanding of natural variability is necessary for establishing robust prediction skill of the ocean carbon sink [Li et al., 2016]. With a moderate ESM ensemble size, it is challenging to conclude whether the number of ensemble members is sufficient to represent the internal variability of the ocean carbon sink. Therefore, using a large ensemble of 100 historical and future scenario simulations based on MPI-ESM, we investigate the variability of ocean carbon uptake by addressing the following questions: (1) Can the ensemble reproduce the occurrence of negative and positive decadal trends in the air-sea CO2 fluxes detected in observations in major carbon sink/source regions? (2) How many ensemble members are required to capture the forced signal over 10 year time-frames?

We find that the internal variability of oceanic carbon uptake is as large as the forced temporal variability, and the largest internal variability is found in major carbon sink regions, i.e., the 50-65°S band of the Southern Ocean, the North Pacific and the North Atlantic.

The MPI-ESM large ensemble produces both positive (i.e., stronger uptake) and negative (i.e., weaker uptake) decadal trends in the ocean carbon uptake in agreement with observations. Negative decadal trends are also projected to occur in the near future.

Due to the large internal variability, the Southern Ocean and the North Pacific require the most ensemble members to reproduce the forced trend. This number varies from decade to decade, and increases from 53 and 46 up to 76 and 79 for the Southern Ocean and the North Pacific in future decades, respectively.

II.2 Future evolution of the ocean carbon uptake variability (in preparation)

The internal variability of the ocean carbon uptake increases significantly when the atmospheric CO2 concentration reaches certain level (840ppmv). The increase of internal variability in the air-sea CO2 flux is aligned with the increase of internal variability of primary production and the mixed layer depth.

Therefore, it is generally fine to assume that the internal variability is stable in contemporary climate states and under moderate atmospheric CO2 concentration growth. However, this assumption of stable internal variability would not apply in a high CO2 world, prone to drastic changes in the physical and biogeochemical regimes of the ocean.

III. Predictability of global carbon cycle and mechanism understanding (in preparation)

The potential predictability, which covers both the forced variability and the internal variability of the Earth System, is found in many ocean regions. Prominent improvement of predictability due to initialisation is found in the North Atlantic, the North Pacific, and the Indian Ocean, is likely related to the large scale oscillations (figure 2.4).

There is potential for establishing predictive skills of ocean carbon uptake against observations.

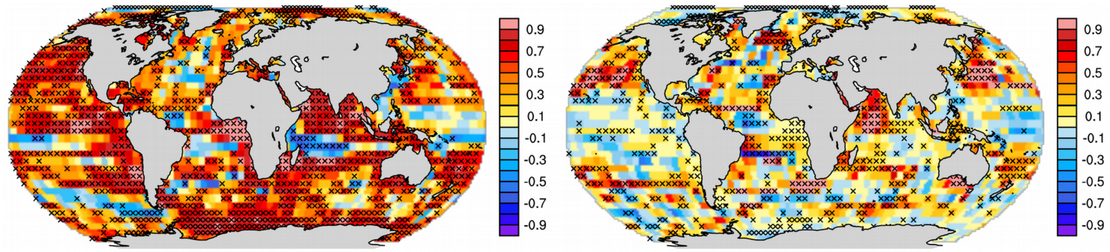

Figure 2.4: Left: Correlation of CO2 flux between assimilation and initialised simulations at lead time of 2-5 from MiKlip baseline 1 simulations. Right: the correlations of uninitialised simulations are subtracted. Potential predictive skill is expressed as the correlation between initialised predictions and assimilation. Crosses denotes significant skills at 95% confidence level. The values were calculated with the MurCSS tool [Illing et al., 2014].

2.5 References

Boer, G. J., et al.: The Decadal Climate Prediction Project, Geosci. Model Dev., 9, 3751-3777, doi:10.5194/gmd-9-3751-2016, 2016.

Drews, A. and Greatbatch, R. J. (2017) The evolution of the Atlantic Multidecadal Variability in a model with an improved North Atlantic Current, J. Climate, doi: 10.1175/JCLI-D-16-0790.1

Eyring, V., Bony, S., Meehl, G. A., Senior, C. A., Stevens, B., Stouffer, R. J., and Taylor, K. E.: Overview of the Coupled Model Intercomparison Project Phase 6 (CMIP6) experimental design and organization, Geosci. Model Dev., 9, 1937-1958, doi:10.5194/gmd-9-1937-2016, 2016.

Fay, A. R., and G. A. McKinley (2013), Global trends in surface ocean pCO2 from in situ data, Global Biogeochemical Cycles, 27(2), 541-557.

Illing, S., C. Kadow, O. Kunst, and U. Cubasch (2014), MurCSS: A Tool for Standardized Evaluation of Decadal Hindcast Systems, Journal of Open Research Software, 2(1), e24.

Kadow, C., et al. (2015) Evaluation of forecasts by accuracy and spread in the MiKlip decadal climate prediction system, Meteorologische Zeitschrift, doi: 10.1127/metz/2015/0639.

Landschützer, P., et al. (2015), The reinvigoration of the Southern Ocean carbon sink, Science, 349(6253), 1221-1224.

Li, H. M., T. Ilyina, W. A. Muller, and F. Sienz (2016), Decadal predictions of the North Atlantic

CO2 uptake, Nature Communications, 7, 11076.

Levitus, S., et al. (1998) NOAA Atlas NESDIS 18, World Ocean Database 1998: vol. 1: Introduction. US Government Printing Office, Washington DC 346.

Schneider, L., Smerdon, J.E., Büntgen, U., Wilson, R.J.S., Myglan, V.S., Kirdyanov, A.V., Esper, J., 2015. Revising midlatitude summer temperatures back to A.D. 600 based on a wood density network. Geophys. Res. Lett. 42, 4556e4562. http://dx.doi.org/10.1002/2015gl063956.

Schuster, U., and A. J. Watson (2007), A variable and decreasing sink for atmospheric CO2 in the North Atlantic, Journal of Geophysical Research-Oceans, 112(C11).

Stoffel, M., Khodri, M., Corona, C., Guillet, S., Poulain, V., Bekki, S., Guiot, J., Luckman, B. H., Oppenheimer, C., Lebas, N., Beniston, M. and Masson-Delmotte, V.: Estimates of volcanic-induced cooling in the Northern Hemisphere over the past1,500 years, Nat. Geosci., 8, 784–788, doi:10.1038/ngeo2526,2015.

Thoma, M., et al. (2015): Decadal hindcasts initialised using observed surface wind stress: Evaluation and Prediction out to 2024, Geophys. Res. Lett., 42 (15), 6454-6461. doi: 10.1002/2015GL064833.

Toohey, M., Stevens, B., Schmidt, H., and Timmreck, C.: Easy Volcanic Aerosol (EVA v1.0): An idealized forcing generator for climate simulations, Geosci. Model Dev., 9(11), 4049–4070, doi:10.5194/GMD-9-4049-2016, 2016

Toohey, M. and Sigl, M.: Volcanic stratospheric sulphur injections and aerosol optical depth from 500 BCE to 1900 CE, Earth Syst. Sci. Data Discuss., https://doi.org/10.5194/essd-2017-31, in review, 2017.

Zanchettin, D., Khodri, M., Timmreck, C., Toohey, M., Schmidt, A., Gerber, E. P., Hegerl, G., Robock, A., Pausata, F. S. R., Ball, W. T., Bauer, S. E., Bekki, S., Dhomse, S. S., LeGrande, A. N., Mann, G. W., Marshall, L., Mills, M., Marchand, M., Niemeier, U., Poulain, V., Rozanov, E., Rubino, A., Stenke, A., Tsigaridis, K., and Tummon, F.: The Model Intercomparison Project on the climatic response to Volcanic forcing (VolMIP): experimental design and forcing input data for CMIP6, Geosci. Model Dev., 9, 2701-2719, doi:10.5194/gmd-9-2701-2016, 2016.

Wilson, R., Anchukaitis, K., Briffa, K.R., Büntgen, U., Cook, E., D'Arrigo, R., Davi, N.,Esper, J., Frank, D., Gunnarson, B., Hegerl, G., Helama, S., Klesse, S., Krusic, P.J.,Linderholm, H.W., Myglan, V., Osborn, T.J., Rydval, M., Schneider, L., Schurer, A.,Wiles, G., Zhang, P., Zorita, E., 2016. Last millennium northern hemisphere summer temperatures from tree rings: Part I: the long term context. Quat. Sci.Rev. 134, 1e18. http://dx.doi.org/10.1016/j.quascirev.2015.12.005.

3. Module C – Regionalisation of Decadal Predictions

Project: **bb0849**
Project title: **MiKlip II Module C – Regionalisation of Decadal Predictions**
Project leader: **Hendrik Feldmann**
Allocation period: **01.01.2017 – 31.12.2017**

3.1 Project overview

MiKlip II module C works on the downscaling of global climate predictions with the regional climate model COSMO-CLM (CCLM). The project aims are to improve the regional prediction system and to provide reliable information about regional decadal predictability for Europe.
The efforts of Module C are an essential contribution to the development of an operational decadal prediction system within in the BMBF funded program MiKlip II. All regionalisation efforts of the research program are bundled within this DKRZ project bb0849.
MiKlip II module C is organised in eight work packages (Cx-WPy), with four WPs requiring considerable computing time at DKRZ, where the other four use these data for analysis and post-processing. The project has currently 19 members of whom 11 participants use the major part of the resources.
Participating institutions are: KIT Karlsruhe, DWD, Goethe University Frankfurt (GUF), University of Cologne and the University of Würzburg

3.2 Main work objectives

The computational work performed within this project at DKRZ can be grouped into four main topics

1. **Ensemble generation (C3-WP3)**: The generation of the core regional decadal ensemble including decadal climate forecasts for the next 10 years using COSMO-CLM. This topic includes also development steps towards an operational use of the prediction system.
2. **Examination of the predictive potential of land surfaces (C1-WP2)**: In this work package the role of land surfaces is explored with respect to the predictability and the potential improvement of the predictive skill from alternative representation of land surface models (LSM) by using other LSM models than the standard model TERRA of CCLM, namely Veg3D and the Community Land Model (CLM) coupled to the CCLM.

3. **Regionally coupled European marginal seas (C1-WP1, C2-WP3)**: Development, testing and application of a regional coupled ocean/atmosphere prediction system using COSMO-CLM and NEMO

Investigation of the European climate variability over centennial time-scales (C2-WP3): This work is intended to improve the attribution of decadal trends to climate variability and change.

3.2.1 Objective 1: Ensemble Generation (WP: C3-WP3)

Contributors: Hans-Jürgen Panitz (KIT), Sascha Brand (DWD), Hendrik Feldmann (KIT)

Main WP Goals

Module C of MiKlip II works on further improving the regional component for the operational use of MiKlip decadal prediction system using the Regional Climate Model (RCM) COSMO-CLM (CCLM), which is the climate version of the operational weather forecast model of the German weather service (DWD), with a regional focus on (Central) Europe. The model domain for the regional decadal simulations of MiKlip II coincides with the domain chosen in MiKlip I, respectively in the frame of EURO-CORDEX (figure 3.2.1a). The horizontal grid-spacing has been fixed to 0.22° (≈25 km).

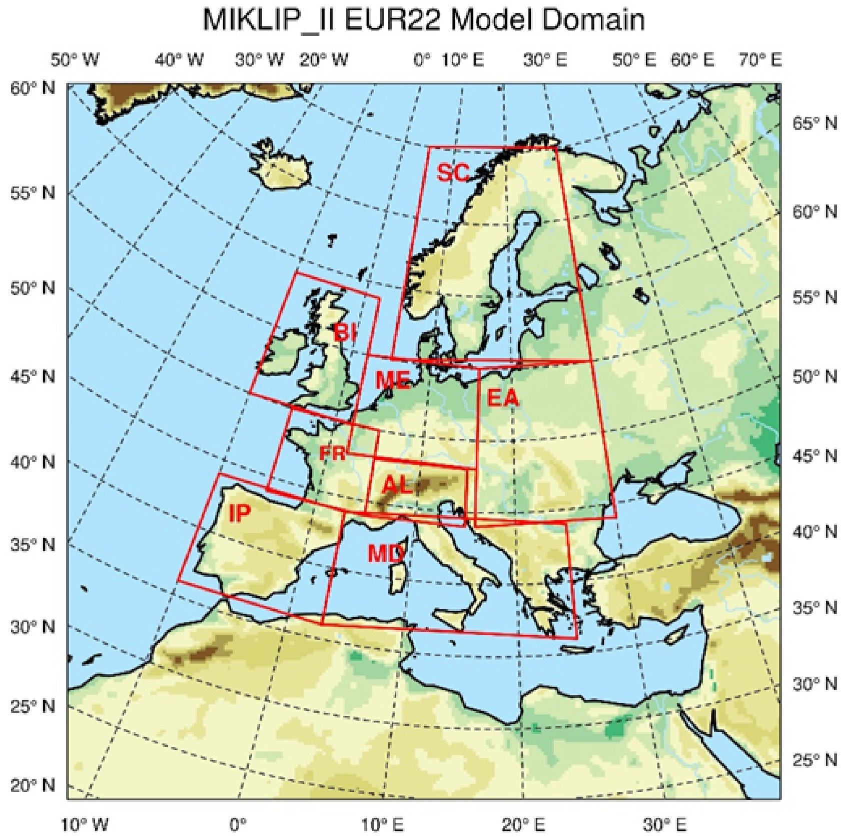

Figure 3.2.1a: Model domain for the decadal simulations using CCLM within MiKlip. Shown are the orography and the location of eight sub-regions generally been used for detailed analyses.

The central task of this work package is to produce an ensemble of regional decadal hindcast simulations using dynamical downscaling with CCLM for the full MiKlip hindcast period from 1960 until the current year (c.f. Figure 1.2). This means about 5700 simulation years for a full hindcast set. Such a large ensemble is necessary to assess the skill of decadal predictions – as they are published on the MiKlip Forecast Web-Page (http://www.fona-miklip.de/decadal-forecast-2017-2026/decadal-forecast-for-2017-2026/). The MiKlip forecasts at the beginning of 2018 will also include the regionalisation results from this project.

The original plan for 2017 was to complete the downscaling of the 4th global hindcast generation "preop". This hindcast generation uses the MPI-ESM-HR as global model with increased resolution. The MPI-ESM results are also intended as a contribution to the CMIP6 Decadal Climate Prediction Project DCPP. Five realisations, using still the CMIP5 external forcing, became available and were downscaled with CCLM in Q4/2016 and Q1/2017. Since there was a delay in the provision of the updated CMIP6 forcing by CMIP, the generation of the new preop members was also delayed until October 2017. MiKlip therefore decided to keep the baseline1 ensemble generation as the basis for the current forecast system. To be able to fulfil the requirement of a complete hindcast data set, this project decided to complete the pre-existing regional baseline1 data set with 5 additional realisations from CCLM and a temporal extension from 2003 until 2016, which amounts to about 300 decadal simulations.

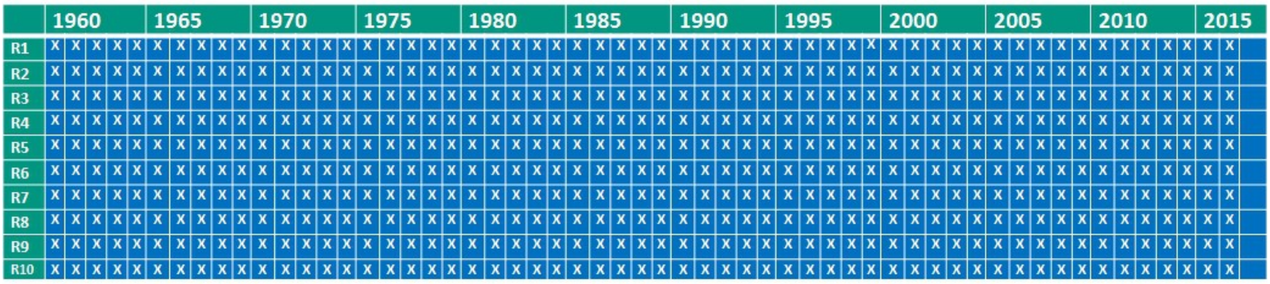

Figure 3.2.1b: Simulation plan for the regional core ensemble. Each X denotes the starting year of a decadal hindcast or forecast simulation. The ensemble includes annual starting dates from 1960 to 2016 (starting dates 1st January of the following year for baseline1 and 1st November for preop). 10 realisations are generated using 1-day shifted starting conditions.

Figures 3.2.1c and 3.2.1d show, why large hindcast ensembles are a prerequisite for a robust skill assessment. Figure 1.3 displays the dependency of the skill estimates – here the Mean Square Error Skill Score (MSESS) – for the regional (CCLM) as well as for the global hindcasts (MPI-ESM-LR) for the ensemble generations baseline0 and baseline1 for the near surface wind (c.f. Reyers et al., 2017). The skill scores increase with the number of ensemble members. The recommendation for the operational prediction system is to use at least 10 members. Note, that there is an added value from the downscaling, since for both generations the skill of CCLM is higher than for MPI-ESM-LR.

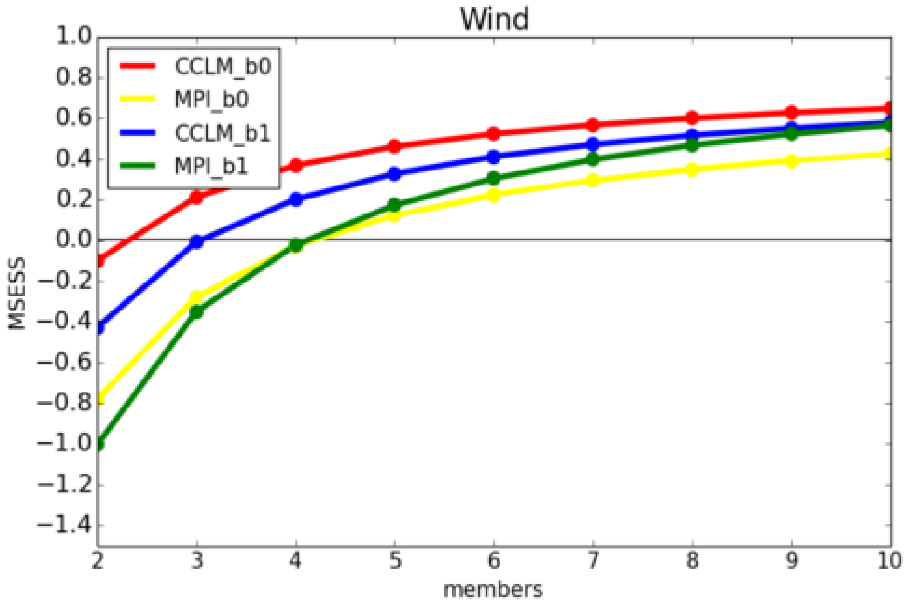

Figure 3.2.1c: Mean Square Error Skill Score MSESS for near surface wind 1960 – 2010 for regional (CCLM) and global (MPI) hindcasts from the baseline0 (b0) and baseline1 ensemble (b1). From: Reyers et al. (2017)

The second prerequisite for robust decadal prediction system is a sufficient number of starting years in the hindcast ensemble. Figure 1.4 shows the MSESS for the near surface temperature in the first forecast year. On the left side the results are shown using five starting years every 10 years (as was available for the first regional hindcast ensemble, e.g. Mieruch et al., 2014). On the right side annual starting dates are used within the analysis. It can be seen, that with annual stating years a significant skill can be achieved over most parts of Europe (note: There are indications that the small areas with negative skill over South Eastern Europe occur probably due to problems in the observational reference E-Obs there). The analysis using the reduced number of starting year displays a patchy pattern with less areas of significant skill.

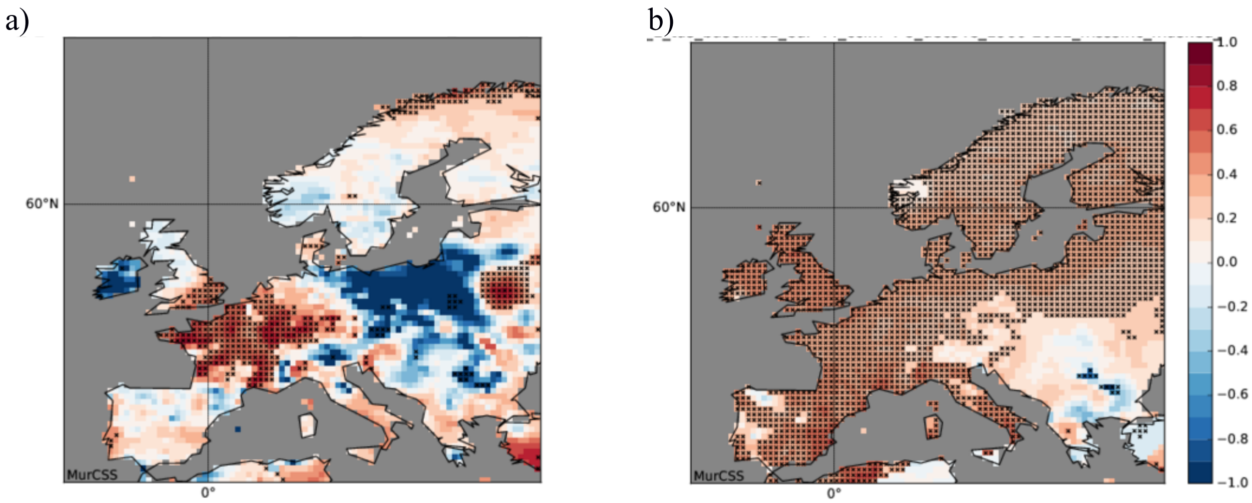

Figure 3.2.1d: MSESS for near surface temperature in the regional MiKlip baseline1 ensemble (10 members) for lead-time year 1. a) starting dates every 10 years, b) 52 annual starting dates from 1960 – 2011. The black dots denote significant skill derived using a bootstrap method.

3.2.2 Objective 2: Predictive potential of land surfaces (WP: C1-WP2)

Contributors: Marcus Breil (KIT), Gerd Schädler (KIT)

The results of MiKlip I showed that the predictive skill of quantities like near surface temperature and precipitation in regional climate predictions is considerably affected by the used Land-Surface Model (LSM) and the soil initialisation. Thus, within work package C1-WP2 in MiKlip II, this predictive potential of land surface processes is further explored by performing and analysing regional decadal hindcast simulations with COSMO-CLM (CCLM) coupled to the alternative LSM VEG3D.

As a first step, a transient stand-alone simulation with VEG3D, driven by ERA-20C reanalysis for the period 1955-2010 was performed to provide balanced soil water and temperature fields for the initialisation of CCLM hindcasts for Europe. Subsequently, within this report period regional decadal hindcasts with CCLM-VEG3D for the decades 1980-2010 are performed, based on these initialisation fields. Figure 2.1a shows the added value (MSESS) of the CCLM-VEG3D simulations compared to the standard CCLM runs (CCLM “preop” core ensemble), using the LSM TERRA, for the anomalies of the monthly precipitation sums in the decades 1980-1989. All simulations are driven by the MPI-ESM-HR realisations 1-5. E-Obs observations are used as reference for both model results. The reddish colours show the areas where the CCLM-VEG3D simulations have an added value, the blue areas where it has none. In central Europe an added value can be recognised for the CCLM-VEG3D simulations, but for a slight majority of the grid cells no added value compared to the standard CCLM-TERRA run can be observed.

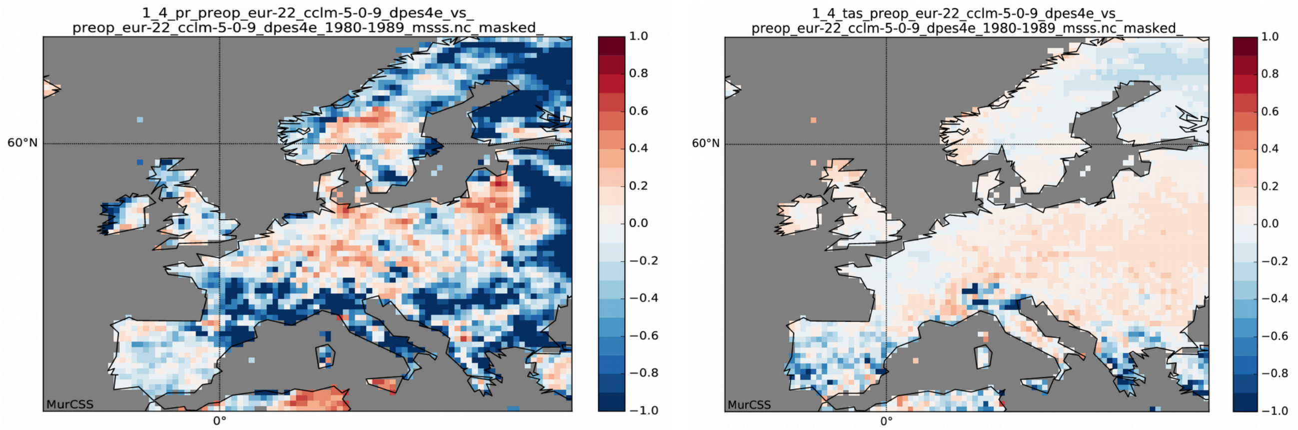

Figure 3.2.2a: Mean Squared Error Skill Score (MSESS) of CCLM-VEG3D compared to CCLM-TERRA for the monthly precipitation sums (a) and the monthly 2m temperatures (b) in the decades 1980-1989 for the realisations 1-5.

In figure 3.2.2a (b), the MSESS of the CCLM-VEG3D simulations compared to the CCLM-TERRA runs for the anomalies of the monthly 2m temperatures are shown. An added value of CCLM-VEG3D can be observed in Central and Eastern Europe as well as for the British Isles for the predicted 2m temperatures. In the Iberian Peninsula and North Scandinavia no added value occurs. One reason for the good performance of CCLM-VEG3D in Eastern Europe are the considerably increased 2m temperatures in winter compared to CCLM-TERRA (Figure 2.3a). Unfortunately, this improvement is caused by an underestimated snow cover, decreasing the albedo values in this area. As a consequence, a bigger amount of solar radiation reaches the surface (Figure 2.3b), leading to a stronger heating of the near surface temperatures in CCLM-VEG3D as in CCLM-TERRA. These increased 2m temperatures, in turn compensate the cold bias in the standard CCLM-TERRA simulations. In the meantime, the underestimation of the snow cover in CCLM-VEG3D could be corrected, but this might lead in further simulations to a reduction of the added value over Eastern Europe.

The analysis of the decadal hindcasts from 1980-1989 for the realisations 1-5 revealed that further model development and tuning of sensitive model parameters in CCLM-VEG3D is necessary. The performance of this optimised model setup and its potential to improve the regional climate predictions compared to CCLM-TERRA will be evaluated in further hindcast simulations for the decades 1990-2010.

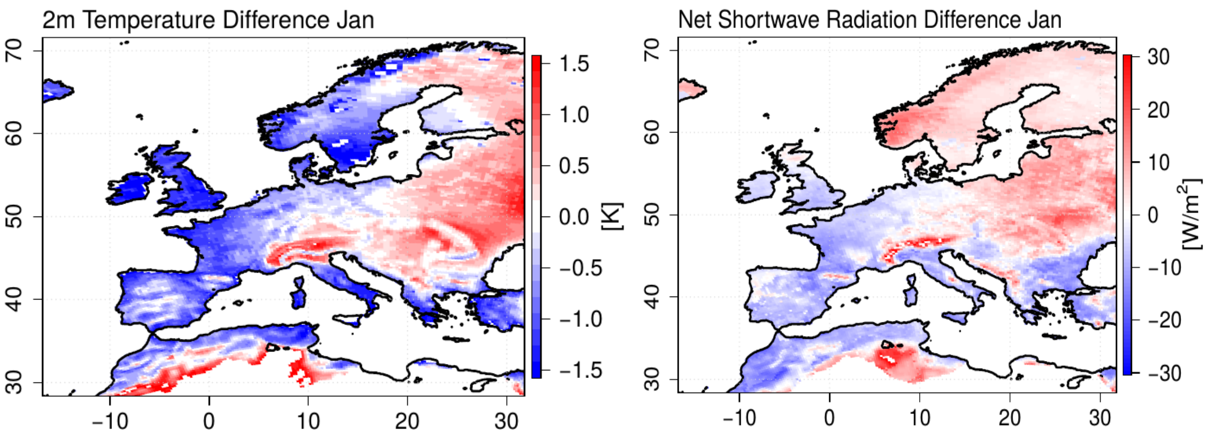

Figure 3.2.2b: Mean differences in January between CCLM-VEG3D and CCLM-TERRA for the monthly mean 2m temperatures (a) and the net shortwave radiation (b) in the decades

Results from this work package are published in: Breil and Schädler (2017), Breil et al. (2017) and Will et al. (2017).

3.2.3 Objective 3: Regionally coupled European marginal seas (WP: C1-WP1, C2-WP3-GUF)

Contributors: Naveed Akhtar, Anika Obermann, Nora Leps, Bodo Ahrens (GUF)

In modules C1-WP1 and C2-WP3, the coupled regional system was developed and tested. It consists of COSMO-CLM, NEMO, TRIP, and OASIS.

During 2017, a coupled system with COSMO-CLM and NEMO-MED (Mediterranean Sea) was tested in terms of its sensitivity to the ocean initial state. 20-year simulations were evaluated with start dates in January and July 1980 and ocean initial fields from Medatlas II. Two simulations were started with the correct month of the climatology; two simulations were started with the climatology of six month later. The impact of the initial state influenced the first six months of the simulation but did not show much impact afterwards.

Furthermore, the centennial simulation with both the Mediterranean and the Northern and Baltic Seas coupled to the atmosphere, was produced. The figure shows the difference in 2m temperature between the coupled and uncoupled system (driven by ERA-Interim SST) for each season. In the coupled system, the Mediterranean Sea is colder in winter and warmer in summer. The North and Baltic Seas are colder in summer. The simulation currently reached the late 1980s.

A simulation with an additional component for the river run-off, TRIP (for Mediterranean basins only), was tested and can be used in decadal forecasts.
Decadal simulations starting in 1930 to 1970 in steps of ten years are currently running.

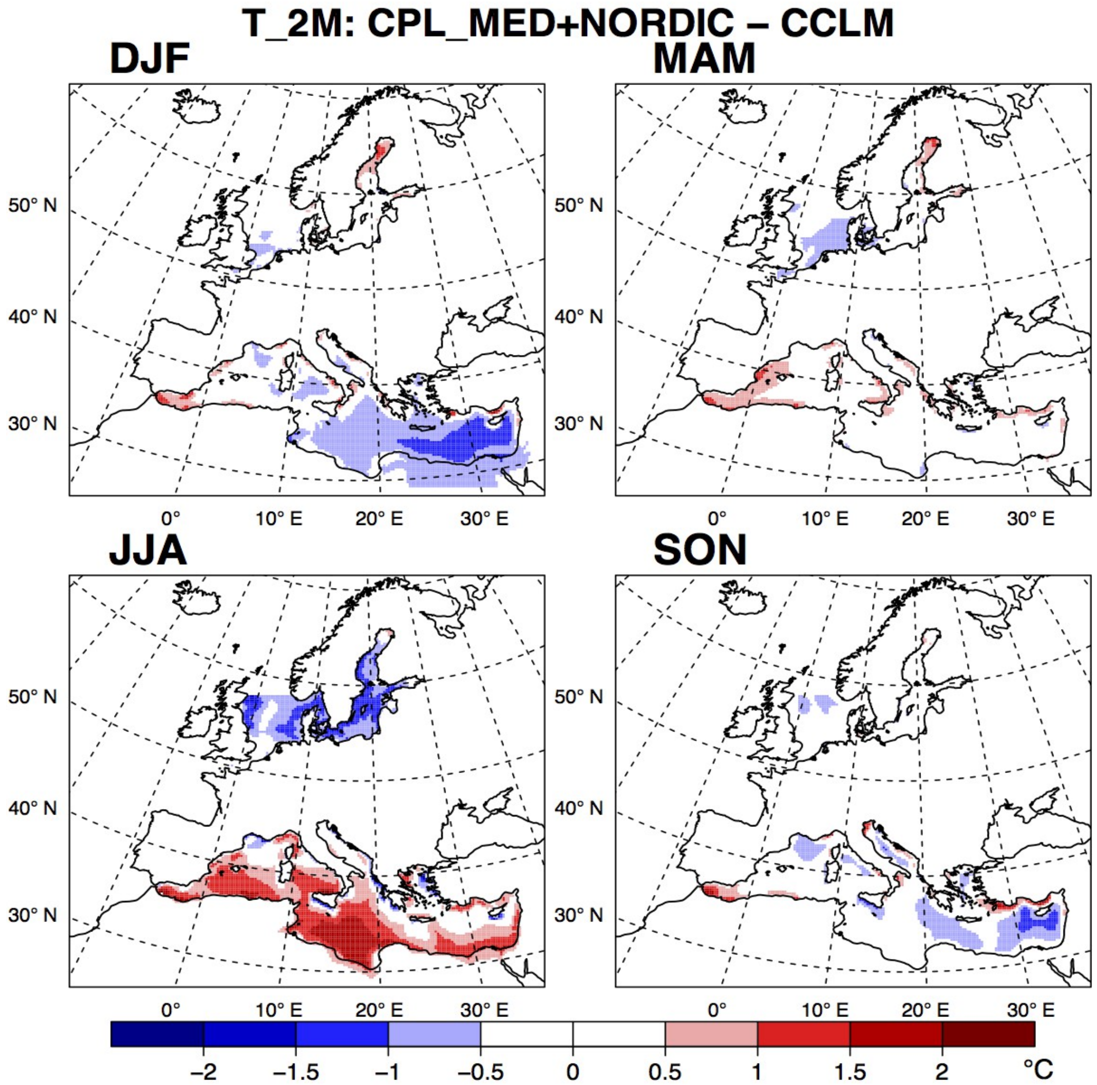

Figure 3.2.3: Near surface temperature – difference between the coupled simulation (CPL) and the un-coupled simulation (CCLM).

Results from this work package have been published in Akhtar et al. (2017), Obermann-Hellhund et al. (2017) and Obermann et al. (2016).

3.2.4 Objective 4: Centennial Hindcasting (WP: C2-WP3)

Contributors: Hendrik Feldmann (KIT), Naveed Akhtar, Bodo Ahrens (GUF)

Climate extreme indices exhibit (multi-)decadal variability or trends. To attribute these signals either to climate change or natural climate variability is uncertain. This attribution is crucial to the aim of MiKlip, because the confidence regarding the expected skill depends on how good the mechanisms behind the predictability are understood.
The historical period covered by reliable observations on the European scale or by CMIP/CORDEX type historical climate simulations usually just covers the second half of the 20th century, at best. But, this period is already strongly affected by the climate trend. Furthermore, the periods are shorter than that of the leading multi-decadal variability indices, like the Atlantic Multi-decadal Oscillation (AMO), which is calculated from de-trended sea-surface temperatures of the North Atlantic. An extension of the examination period provides valuable information.

A set regional downscaling for Europe has been performed with CCLM to cover the whole 20th century (simulation period 1900 – 2010, c.f. Table 3.2.4) by downscaling MPI-ESM global simulations and ERA20C (in collaboration with the DKRZ project bb0983). These simulations improve the coverage of different phases of the AMO and other climate variability pattern and their impact on the European climate. The atmosphere only simulations are completed since end of September 2017. The generation of simulations with the coupled ocean is ongoing.

Figure 3.2.4 shows, that the centennial hindcasts show a high correlation with the available observations, as well for mean temperature as for daily maximum temperature and other variables (not shown).

Results of the Work package have been published in Kottmeier and Feldmann (2017). Further publications are in preparation.
We thank DKRZ for providing the computing resources for these studies.

Table 3.2.4: List of 20th century (centennial) downscaling experiments with the uncoupled standard CCLM- In total: 3834 simulation years

	Name	Experiment	Period	Type
1	as08ncep	20CR via MPI-ESM-LR	1900-2009	Reference
2	as22ncep	20CR via MPI-ESM-LR	1900-2009	Reference
3	as26ncep	20CR via MPI-ESM-LR	1900-2009	Reference
4	CCLM_ERA20C	ERA20C	1900-2010	Reference
5	historicalext_ r1i1p1-HR	MPI-ESM-HR Historical R1	1900-2030	Un-initialised historical
6	historicalext_ r2i1p1-HR	MPI-ESM-HR Historical R2	1900-2030	Un-initialised historical
7	historicalext_ r3i1p1-HR	MPI-ESM-HR Historical R3	1900-2030	Un-initialised historical
8	dec08oXXXX	MPI-ESM-LR DROUGHTCLIP	1910 – 2009 100 decades	Decadal hindcasts
9	dec22oXXXX	MPI-ESM-LR DROUGHTCLIP	1910 – 2009 100 decades	Decadal hindcasts
10	dec26oXXXX	MPI-ESM-LR DROUGHTCLIP	1910 – 2009 100 decades	Decadal hindcasts

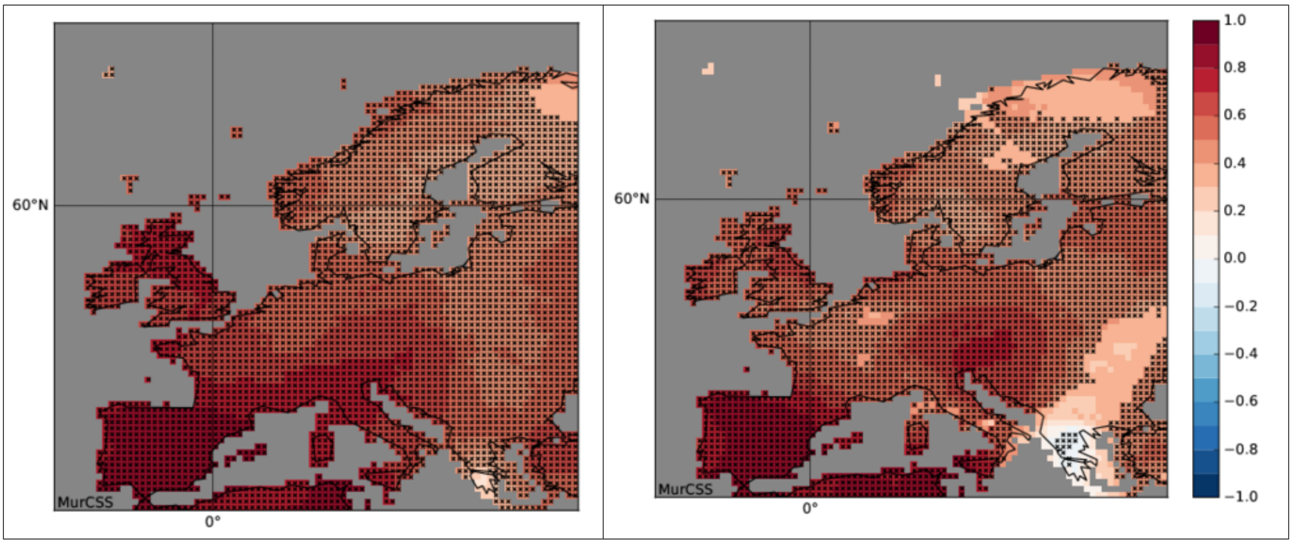

Figure 3.2.4: Anomaly correlation of the near-surface temperature between the centennial hindcasts lead-time year 2-5 and the CRU TS4.01 observations for the period 1912 – 2014. Left: for daily mean temperature; right: for daily maximum temperature.

3.3 Project publications with DKRZ acknowledgements

Akhtar, N., J. Brauch, B. Ahrens (2017). Climate Modeling over the Mediterranean Sea: Impact of Resolution and Ocean Coupling. Climate Dynamics. DOI 10.1007/s00382-017-3570-8 (OA).

Breil, M., G. Schädler, 2017: Quantification of the uncertainties in soil and vegetation parameterizations for regional climate simulations in Europe. Journal of Hydrometeorology, 18 (5), 1535–1548. doi:10.1175/JHM-D-16-0226.1.

Breil, M., Panitz, H.-J., Schädler, G. (2017): Impact of the soil-vegetation-atmosphere interactions on the spatial rainfall variability in the Central Sahel. Meteorologische Zeitschrift, doi:10.1127/metz/2017/0819.

Kottmeier, Ch., Feldmann (2017): Regionale dekadische Klimavorhersagen und nahtlose Vorhersagen. PROMET Heft 99, 57-64.

Marotzke J. W. A. Müller, F.S.E. Vamborg, P. Becker, U. Cubasch, H. Feldmann, F. Kaspar, Ch. Kottmeier, C. Marini, I. Polkova, K. Prömmel, H.W. Rust, D. Stammer, U. Ulbrich, C. Kadow, A. Köhl, J. Kröger, T. Kruschke, J.G. Pinto, H. Pohlmann, M. Reyers, M. Schröder, F. Sienz, C. Timmreck, and M. Ziese (2016): MiKlip - a National Research Project on Decadal Climate Prediction. Bull. Amer. Meteor. Soc., 97, 2379–2394.

Mieruch, S., H. Feldmann, G. Schädler, C. J. Lenz, S. Kothe, and Ch. Kottmeier (2014): The Regional MiKlip Decadal Forecast Ensemble for Europe: the Added Value of Downscaling., Geosci. Model Dev., 7(6), 2983-2999, doi:10.5194/gmd-7-2983-2014.

Moemken J, Reyers M, Buldmann B, Pinto JG (2016): Decadal predictability of regional scale wind speed and wind energy potentials over Central Europe. Tellus A, Vol. 68 (29199).

Obermann-Hellhund, A., D. Conte, S. Somot, C. Zsolt Torma, B. Ahrens (2017). Mistral and Tramontane wind systems in regional and global climate simulations from 1950 to 2100. Climate Dynamics. DOI: 10.1007/s00382-017-3635-8.

Obermann, A., S. Bastin, S. Belamari, D. Conte, M. A. Gaertner, L. Li, B. Ahrens (2016). Mistral and Tramontane wind speed and wind direction patterns in regional climate simulations. Climate Dynamics. doi:10.1007/s00382-016-3053-3 (OA).

Paeth, H., Paxian, A., Sein, D., Jacob, D., Panitz, H.-J., Warscher, M., Fink, A., Kunstmann, H., Breil, M., Engel, T., Krause, A., Toedter, J., Ahrens, B. (2015): Decadal and multi-year predictability of the West African monsoon and the role of dynamical downscaling. J. Clim., submitted.

Paxian, A., Sein, D., Panitz, H.-J., Warscher, M., Breil, M., Engel, T., Toedter, J., Krause, A., Cabos Narvaez, W. D., Fink, A. H., Ahrens, B., Kunstmann, H., Jacob, D., Paeth, H. (2016): Bias reduction in decadal predictions of West African monsoon rainfall using regional climate models. J J. Geophys. Res. Atmos., Vol. 121 (4), pp. 1715–1735.

Weimer, M., Mieruch, S., Schädler, G., Kottmeier, Ch. (2016): A new estimator of heat periods for decadal climate predictions – a complex network approach. Nonlin. Processes Geophys., 23, 307-317, doi:10.5194/npg-23-307-2016.

Will, A., Akhtar, N., Brauch, J., Breil, M., Davin, E., Ho-Hagemann, H., Maisonnaive, E., Thürkow, M., Weiher, S. (2017): The regional climate model and the model components coupled via OASIS3-MCT: description and performance. Geoscientific Model Development , 10 (4), 1549–1586. doi:10.5194/gmd-10-1549-2017

4. Module D – Synthesis

Project: **bm0807**
Project title: **MiKlip II Module D – Synthesis**
Old title during MiKlip first phase (**A flexible forecast system for decadal climate predictions - FLEXFORDEC)**
Project lead: **Jochem Marotzke**
Reporting period: **01.01.2017 – 31.10.2017**

4.1 Project overview

Module D is responsible for developing the global decadal climate prediction system and the accompanying central evaluation system, the transfer of the system to DWD, and the setting up of pilot studies for the application of decadal predictions by government agencies and by the private sector. The project consortium consists of 4 project partners and is described in the CPU request for 2016 and 2017.

Strategically, MPI-M leads the coordination of MiKlip II and Module D, with the overall project being led by J. Marotzke, the scientific and technical implementation being led by W. Müller, and the MiKlip Office being led by S. Hettrich. MPI-M takes the lead in the development of the global prediction system and supports the transfer of the global model to operational use (**FLEXFORDEC**). FUB takes the lead in the development of the central evaluation system (**INTEGRATION**), hosted on the MiKlip Server. FUB also supports DWD in the transfer of the evaluation system for operational use of global decadal climate predictions. DWD implements both the global prediction and the central evaluation system on their local machines for operational use (**OPERATIONS**). Moreover, DWD provides a pilot study for the use of decadal predictions for government agencies (**SUPPORT**) and GERICS provides a pilot study for the use of decadal predictions for the private sector (**IPRODUCTS**).

In addition to the MiKlip II project objectives, **FLEXFORDEC** also coordinates the MPI-M contribution to the CMIP6 decadal predictions (organised by the WCRP Decadal Climate Prediction Project (DCPP) with W. Müller as a member, Boer et al. 2016) and takes the responsibility for providing the CMIP6 DECK experiments for the high-resolution version of the MPI-ESM (MPI-ESM-HR, Müller et al., 2017). MiKlip is also partner of the WCRP Grand Challenge on Near Term

Climate prediction (with W. Müller as a member, Kushnir et al., 2017). Their overall objectives are the production of standards, verification methods and guidance for near term predictions in collaboration with the WMO Commission for Basic Systems / Commission for Climatology (CBS/CCL) Expert Team, the achievement of WMO recognition for operational decadal predictions, and the initiation and issuance of a real-time Global Decadal Climate Outlook once each year in consultation with CBS/CCL and following the template of the Global Seasonal Climate Update (GSCU) for seasonal predictions.

MiKlip II Module D develops and provides the decadal prediction and evaluation systems of MiKlip II. As such the project is responsible for providing all project partners with the newest central simulations of the prediction system. MiKlip II Module D will also provide the Max Planck Institute for Meteorology's contribution to the DCPP of CMIP6. The main model used for the MPI-M CMIP6 simulations and for MiKlip is the MPI-ESM in its low and high resolutions (LR and HR). The MiKlip II Module D project has taken on the responsibility for setting up the MPI-ESM-HR (atmosphere: T127L95, ocean: TP04L40) for CMIP6.

The decadal hindcasts of the central prediction system and the DECK experiments are performed with the coupled model ECHAM6/MPIOM in high resolution, MPI-ESM-HR (T127L95/TP04L40). The model is already implemented in the DKRZ HPC infrastructure Mistral. MPI-ESM-HR is well tuned and a description of the model, its tuning and results is in preparation (Müller et al. 2017). Climate sensitivity is ~3K and similar to MPI-ESM-LR. The atmospheric global mean surface temperature exhibits no drift and stays on the target value of 13.8°C. The drift of global mean ocean temperature and salinity exhibits only little magnitudes and are comparable to earlier version of MPI-ESM-LR. The Atlantic meridional overturning at 26°N has a value of 16SV on time-average and is comparable to observational estimates. This shows that the coupled model is in a stable state. The CMIP5 forcing is similar to the forcing applied in previous versions of MPI-ESM such as described in Giorgetta et al. (2013). For CMIP6 major changes include the use of MAC-v2-SP for the anthropogenic tropospheric aerosols, new ozone data, a slightly lower value of total solar irradiation (~1360W/m2) and a new land-use data (LUH2).

4.2 Completing DECK and decadal hindcast simulations with CMIP5 forcing

FLEXFORDEC has performed DECK simulations with CMIP5 forcing. This set-up rose from the fact that CMIP6 forcing only has become available in 2017. **FLEXFORDEC** has increased the ensemble size of the historical simulations to 10 ensemble members and performed a set of decadal MiKlip II hindcasts. For the set-up of the decadal hindcasts, it was decided by the MiKlip steering group to use reanalysis data from ERA40/ERAinterim for initialising the atmosphere and temperature and salinity anomalies from ORA-S4 for the ocean initialisation. Additionally, a new sea-ice assimilation was implemented following the suggestions of the steering group. The output variables list was updated in accordance to the DCPP variable list, extended by needs of the MiKlip partners. The performance of the decadal hindcasts is currently evaluated (figure 4.2).

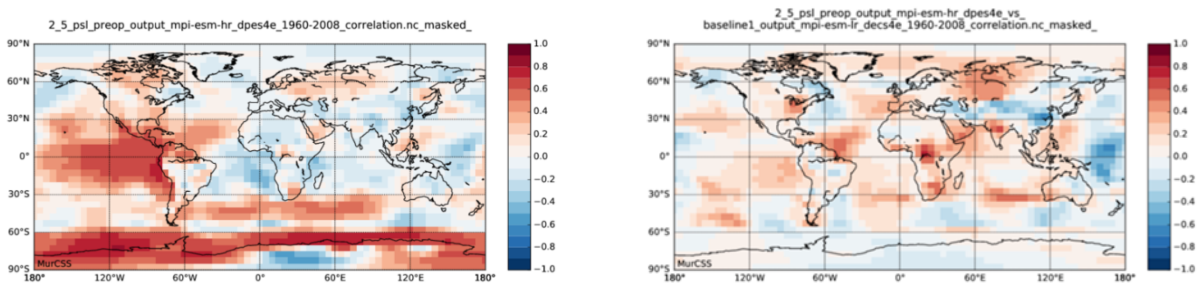

Figure 4.2: Correlation skill of sea level pressure for lead years 2-5 of the preoperational-HR system (mean of 5 ensemble members) with CMIP5 forcing (left) and the difference to the baseline1-LR system (right).

4.3 Implementing the CMIP6 forcing and producing DECK simulations

FLEXFORDEC is in charge of providing the CMIP6 DECK experiments for MPI-ESM-HR. The CMIP6 forcing is now available and, in association with the MPI contribution to CMIP6, the DECK experiments need to be repeated with the CMIP6 forcing. An extended spin-up of the control run was necessary in order to tune the sea-ice properties of the model and additionally to reach an acceptable equilibrium in the sedimentation rate of the HAMOCC component. This run was followed by the CMIP6 DECK experiments (control run, 1% CO2 increase, abrupt 4 x CO2 and 5 historical runs) for MPI-ESM-HR. These simulations are now successfully completed. The increase of the ensemble size of 10 historical run are planed together with the DKRZ CMIP6 project (S. Legutke)

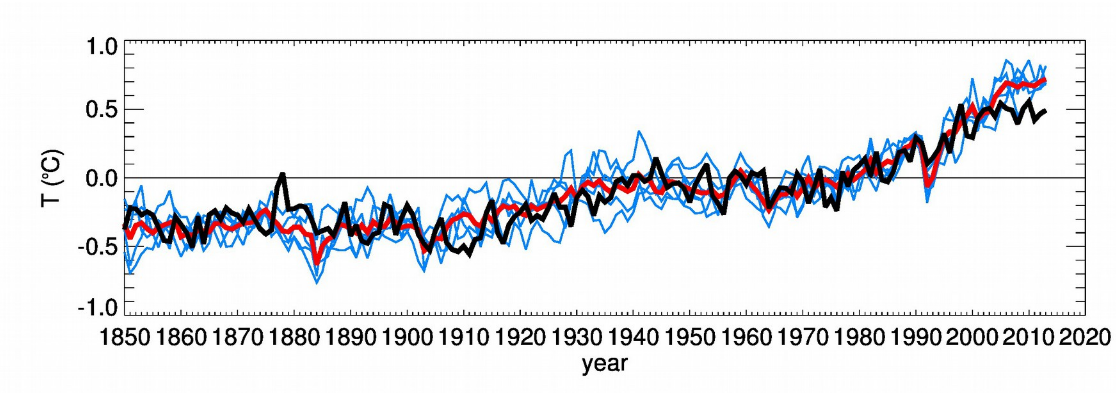

Figure 4.3: Global mean temperature anomalies from observations (black), the 5 historical-HR simulations (blue) and their ensemble mean (red).

4.4 Assimilation run and decadal hindcast simulations with CMIP6 forcing

Decadal hindcasts are a fundamental contribution to CMIP6 within DCPP (Boer et al., 2016). The use of CMIP6 forcing is essential as new updates in aerosol and volcanic forcing are implemented and the forcing is extended until 2015. Repeating the hindcasts with CMIP6 forcing is mandatory. A minimum of 10 ensemble members yearly initialised hindcasts is required for the current system, because this number has been shown to be necessary in order to achieve robust skill estimates for the North Atlantic, but also in order to fulfil the requirements of the CMIP6 decadal MIP.

As a first step to get the starting fields for the decadal hindcast simulations, an assimilation run was performed. The assimilation run is similar to the previous one performed with CMIP5 forcing. Atmospheric temperature, vorticity, divergence and pressure data were nudged towards data from ERA40/ERAinterim reanalysis. Since a newer version of the ECMWF ocean reanalysis ORA-S5, covering the period after 1979, has become available a combination of ORA-S4 and ORA-S5 was used for nudging ocean temperature and salinity anomalies. Since the sea ice properties in ORA-S5 have improved to the previous version (Chevallier et al. 2016) we use these data now for nudging the sea ice concentration anomalies. As in the system with CMIP5 forcing a statistical relation between sea-ice concentration and sea-ice thickness is used (Tietsche et al. 2012). Starting from the initial conditions of the assimilation run we have started to produce decadal hindcast simulations with CMIP6 forcing.

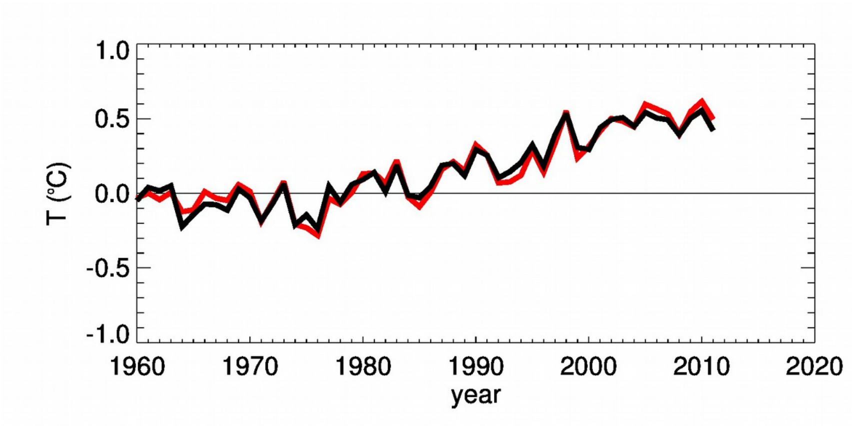

Figure 4.4: Global mean temperature anomalies from observations (black) and the assimilation run (red).

4.5 Ensemble Dispersion Filter Experiments with MPI-ESM-1.2 and Preop-LR

INTEGRATION investigates a new re-initialisation method called ensemble dispersion filter (EDF). Here, individual members of the hindcasts are rescaled to the ocean state of the ensemble mean (details in Kadow et al. 2017). In 2017 the EDF was adapted to the MPI-ESM1.2, taking part in an assessment of new methods for MiKlip organised for MiKlip-Module A. With the new model system, 10 members, in the longer time frame 1960-2016 the EDF still boosts the prediction skill of its reference system up to 5 years ahead (Fig. 4). The skill scores show improvements in the climate-relevant regions of the Central and North Pacific, and the North Atlantic for 2m temperature. Other climate diagnostics like ocean heat content support these results (not shown). Due to the long assembling time to get the EDF within the new MPI-ESM1.2, more node hours were necessary to test the system for the MiKlip Module A assessment, which only requested up to 5 lead years. The longer runs up to 10 years are postponed. However, as the main boost-effects happen in the later lead years (4 and 5), probably the improvements are even stronger in the later stages (LY6-10). With the new stable version of the EDF further analysis will be done in the future.

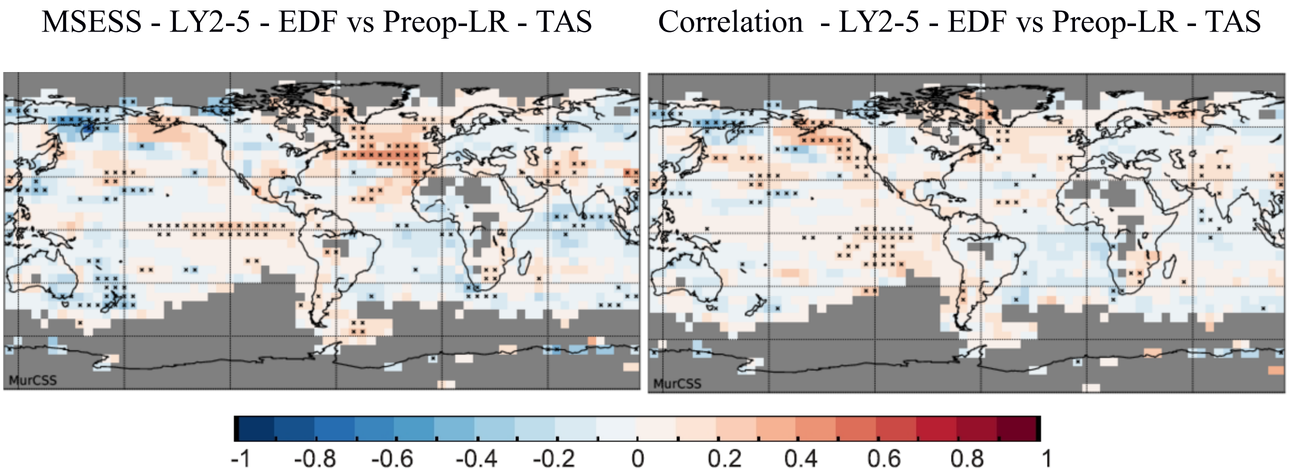

Figure 4.5: Mean Squared Error Skill Score (left) and Correlation (right) of the EDF with the Preop-LR as reference – each as a 10 ensemble member system. Near Surface Air Temperature is analysed in the lead years 2 to 5 hindcast compared to HadCRUT4. Significant differences are marked by crosses. Gray areas mark missing values with less than 90% data consistency in the observation. The analyses cover the time period from 1962 to 2016.

4.6 Computing time

1203000 node hours were granted for MiKlip II Module D in 2017. These were shared according to 20%, 20%, 30% and 30% during the four quarters of 2017, i.e. 240 T., 240 T., 361 T. and 361 T. Almost all of the allocated computing time for 2017 has been consumed until today.

Table 4.6: Overview of the experiments undertaken with MPI-ESM-HR and to test the Ensemble Dispersion Filter (EDF) with MPI-ESM-LR and estimated computing time.

Experiment	Model years (node hours)	Used in Quarter
Hindcast CMIP5 (Ens-mem 4 & 5)	900 (165 Thousand)	Q1
6 x Historical (CMIP5 forcing)	6 x 150 (175 T.)	Q1, Q2, Q3
Control-Spin-up	1 x 1200 (220 T.)	Q2, Q3
Control	500 (90 T.)	Q3
5 x Historical (CMIP6 forcing)	5 x 150 (140 T.)	Q3
Assimilation	2 x 60 (20 T.)	Q3
1% CO2	150 (30 T.)	Q4
Abrupt 4 x CO2	150 (30 T.)	Q4

Hindcast CMIP6 (Ens-mem 1 & 2)	2x600 (300 T.)	Q4
EDF 10 member (Preop-LR)	4.200 (100 T)	Q2,Q3,Q4
Expired	(11 T., 0, 24 T.) 5 %, 0 %, 6 %	Q1, Q2, Q3

4.7 References

Boer, G. J. and Smith, D. M. and Cassou, C. and Doblas-Reyes, F. and Danabasoglu, G. and Kirtman, B. and Kushnir, Y. and Kimoto, M. and Meehl, G. A. and Msadek, R. and Mueller, W. A. and Taylor, K. E. and Zwiers, F. and Rixen, M. and Ruprich-Robert, Y. and Eade, R., 2016, The Decadal Climate Prediction Project (DCPP) contribution to CMIP6, Geosci. Model Dev., 9, 3751-3777, 2016

Chevallier, M., Smith, G. C., Dupont, F., Lemieux, J.-F., Forget, G., Fujii, Y., et al. (2016). Intercomparison of the Arctic sea ice cover in global ocean–sea ice reanalyses from the ORA-IP project. Climate Dynamics. http://doi.org/10.1007/s00382-016-2985-y

Giorgetta, M. A., Jungclaus, J. H., Reick, C. H., Legutke, S., Brovkin, V., Crueger, T., Esch, M., Fieg, K., Glushak, K., Gayler, V., Haak, H., Hollweg, H.-D., Ilyina, T., Kinne, S., Kornblueh, L., Matei, D., Mauritsen, T., Mikolajewicz, U., Mueller, W. A., Notz, D., Raddatz, T., Rast, S., Redler, R., Roeckner, E., Schmidt, H., Schnur, R., Segschneider, J., Six, K., Stockhause, M., Wegner, J., Widmann, H., Wieners, K.-H., Claussen, M., Marotzke, J., & Stevens, B. (2013). Climate and carbon cycle changes from 1850 to 2100 in MPI-ESM simulations for the coupled model intercomparison project phase 5. Journal of Advances in Modeling Earth Systems, 5, 572-597

Kushnir, Y., A. A. Scaife, R. Arritt, G. Balsamo, G. Boer, D. Carlson, F. Doblas-Reyes, E. Hawkins, M. Kimoto, A. Kumar, D. Matei, K. Matthes, W. A. Müller, T. O'Kane, J. Perlwitz, S. Power, M. Raphael, A. Shimpo, M. Tuma, M. Sparrow and Doug Smith, 2017: Near-Term Climate Prediction (in preparation)

Müller, W. A. et al, 2017: A high resolution version of the Max-Planck Institute Earth System Model (MPI-ESM-HR), JAMES (in preparation)

5. Module E – Evaluation of the MiKlip Decadal Prediction System

Project: **bb0763**
Project title: **MiKlip II Module E – Evaluation of the MiKlip Decadal Prediction System**
Project lead: **Marc Schröder, Thomas Spangehl**
Reporting period: **01.01.2017 – 31.12.2017**

5.1 Description of work and summary of results

The PROVESIMAC project focuses on the evaluation of the decadal climate prediction system developed within the second phase of MiKlip (research programme funded by Federal Ministry of Education and Research in Germany, BMBF, http://www.fona-miklip.de/) utilising satellite data. Satellite simulators for usage with MPI-ESM are developed for the Special Sensor Microwave Imager (SSM/I) and for the Special Sensor Microwave Imager and Sounder (SSMIS) utilising the CFMIP Observation Simulator Package (COSP, Bodas-Salcedo et al., 2011).

The COSP SSM/I satellite simulator is applied to the MiKlip II pre-operational hindcasts to evaluate the climatological and predictive skill of the system. Simulated brightness temperatures for selected channels which are sensitive to water vapour content and to precipitation are used. On the reference side the SSM/I & SSMIS Fundamental Climate Data Record (FCDR) provided by the CM SAF (DOI: 10.5676/EUM_SAF_CM/FCDR_MWI/V003) is used which covers the period from 1978 to 2015. The presented evaluation results focus on lead years 1-3 and are restricted to the period 1996-2008 but the analysis is currently extended to cover the full observational period.

The brightness temperature of the 22 GHz channel is sensitive to water vapour content whereas the difference of the 85 GHz vertical minus horizontal polarisation channel (pv-ph) is sensitive to the hydrometer content. Results obtained for the COSP SSM/I satellite simulator applied to the MiKlip II pre-operational system resemble the general structure and amplitude of the observations for multi-year time averages for both channels. Over the central equatorial Pacific there is evidence for a double ITCZ structure which is a common feature of GCMs (figure 5.1.1).

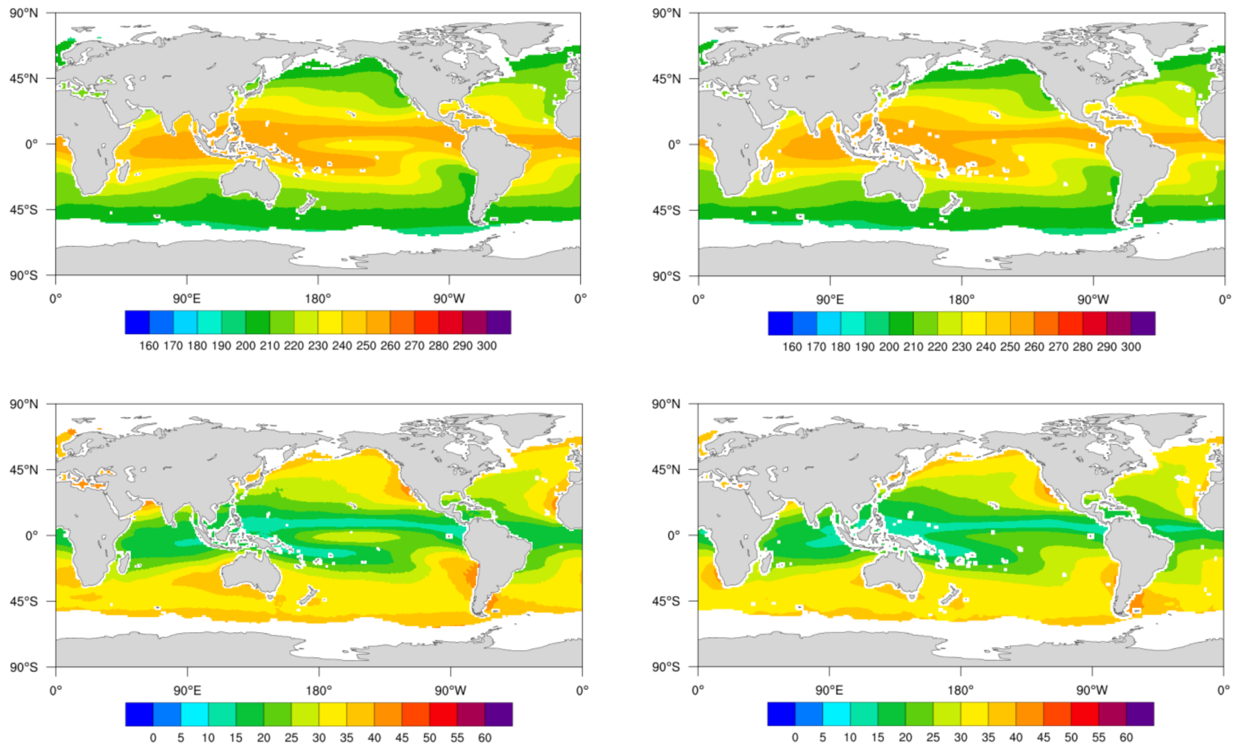

Figure 5.1.1: Brightness temperature [K] multi-year averages (1996-2008) of the SSM/I microwave imager for the 22 GHz channel (top) and the 85 GHz vertical minus horizontal polarisation channel (bottom). Left column shows results of the COSP SSM/I satellite simulator applied to the MiKlip II pre-operational system (lead year 1). Right column shows observations. Land areas are masked out due to lack of surface information.

Probabilistic evaluation results are shown for the 85 GHz (pv-ph) channel. For lead year 1 analysis of variance (ANOVA) reveals potential predictability for large parts of the tropical ocean areas. The Conditional Ranked Probability Skill Score (CRPSS) indicates predictive skill for large parts of the tropical/sub-tropical Pacific, parts of the tropical/sub-tropical Atlantic and the equatorial Indian Ocean. No predictive skill is found for the eastern equatorial Pacific suggesting that the area of maximum potential predictability in the equatorial eastern Pacific is related to an underestimation of the hindcast spread in this area. For lead years 2-3 ANOVA still indicates potential predictability for equatorial ocean areas. Moreover, CRPSS indicates predictive skill for large parts of the tropical/subtropical ocean areas including the ITCZ and south Pacific convergence zone in the Pacific, parts of the Indian Ocean and large parts of the tropical/subtropical North Atlantic. These results suggest that the hindcasts show skill even beyond lead year 1 when comparing against climatology as a reference forecast.

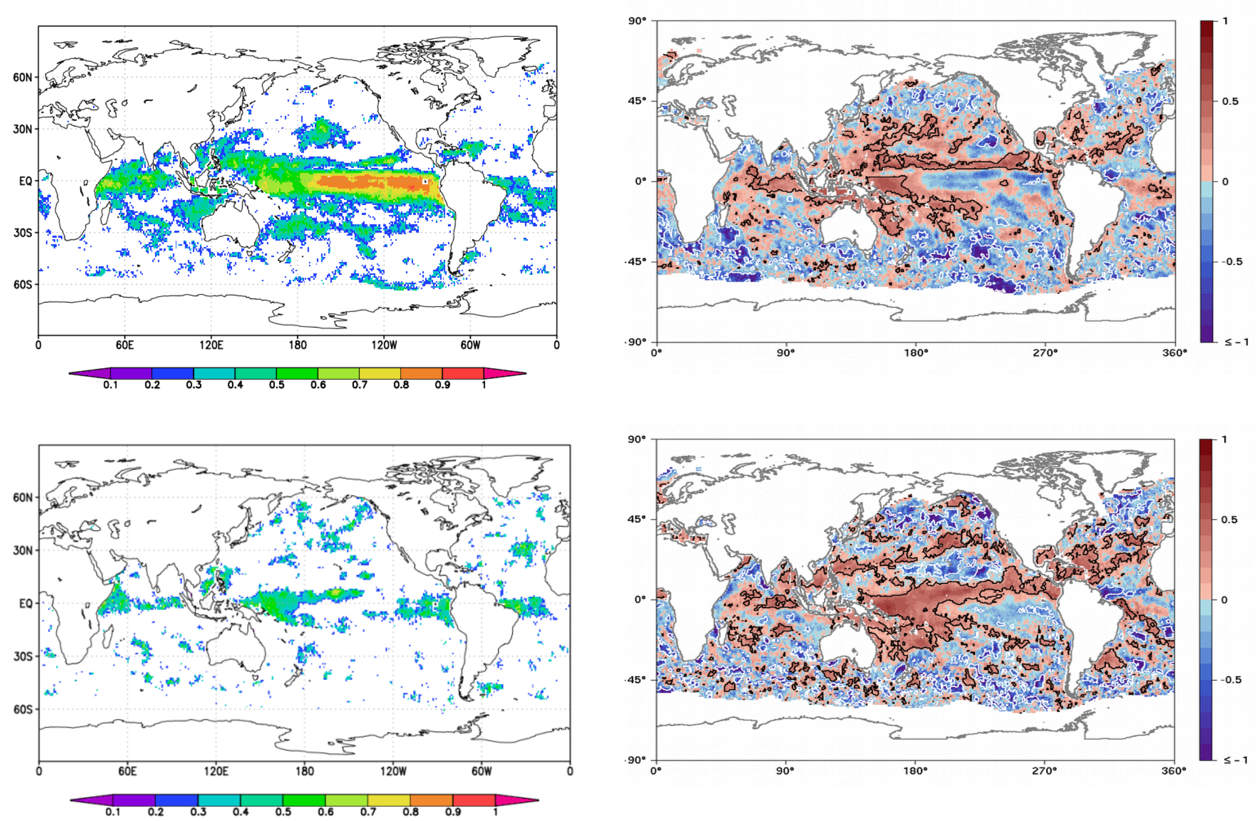

Figure 5.1.2: MiKlip II pre-operational system forecast evaluation of brightness temperature for the 85 GHz vertical minus horizontal polarisation channel for (top) lead year 1 and (bottom) lead year 2-3. Left column shows ANOVA and right column shows CRPSS. Land areas are masked out due to lack of surface information. The covered time period is 1996-2006. 4 realisations are used.

5.2 References

Bodas-Salcedo, A., and Co-authors, 2011: COSP: Satellite simulation software for model assessment. Bull. Amer. Meteor. Soc., 92, 1023-1043, doi: http://dx.doi.org/10.1175/2011BAMS2856.1.